coatings

MDPI

Article

The Use of Polyurethane Composites with Sensing Polymers as New Coating Materials for Surface Acoustic Wave-Based Chemical Sensors—Part III: Ultrasonic Analyses and Optical Microscopy Characterization of the Coating Results

Mauro dos Santos de Carvalho [1,*], Michael Rapp [2,*], Achim Voigt [2] and Marian Dirschka [2]

[1] Chemistry Institute, Federal University of Rio de Janeiro, Rio de Janeiro 21941-909, Brazil
[2] Institute of Microstructure Technology, Karlsruhe Institute for Technology, 76344 Eggenstein-Leopoldshafen, Germany
* Correspondence: mauro@iq.ufrj.br (M.d.S.d.C.); michael.rapp@partner.kit.edu (M.R.)

Abstract: The chemical sensitization of surface acoustic wave (SAW) sensors plays a key role for this technology. The analysis of the resulting nanometric sensing layer is crucial for the development of new sensing materials as well as for the quality control of SAW sensors systems for commercial applications. In the previous works, the resulting coating layers using new coating materials based on polyurethane-polymer composites were evaluated considering the ultrasonic analysis, the adhesion, and the sensor responses. In this work, the characterization of the coating process, Bright Field Microscopy (BFM) and Dark Field Microscopy (DFM) were used to evaluate the quality of the material distribution and homogeneity of the obtained sensing layers. The sensing materials analyzed were the four polymers used in the previous works and their respective new composites with polyurethane (PU). The combination of BFM and DFM allows the characterization of the resulting material distribution obtained by the coating process, providing inferences about the interaction of each coating material with the surface of the SAW sensor element as well as about the correlation between the results of the ultrasonic parameters, the real material distribution and the homogeneity of the obtained coating layer of each coating material.

Keywords: polymeric sensing layer; layer deposition; coating layer structure; polymeric thin film

Citation: Carvalho, M.d.S.d.; Rapp, M.; Voigt, A.; Dirschka, M. The Use of Polyurethane Composites with Sensing Polymers as New Coating Materials for Surface Acoustic Wave-Based Chemical Sensors—Part III: Ultrasonic Analyses and Optical Microscopy Characterization of the Coating Results. *Coatings* **2024**, *14*, 846. https://doi.org/10.3390/coatings14070846

Academic Editors: Nicolas Delorme and Guillaume Vignaud

Received: 29 May 2024
Revised: 24 June 2024
Accepted: 2 July 2024
Published: 5 July 2024

1. Introduction

Chemical sensors based on the detection and analysis of surface acoustic wave (SAW) propagation over a piezoelectric substrate has been developed over the two past decades [1,2]. This type of chemical sensor has been studied due to its versatility, low cost, and high sensibility.

The performance of the SAW technology relies on two principal factors: first is the hardware and its respective electronic design, which is responsible for the quality of the electronic transduction and the stability and precision of the signal of the sensor response. The second factor relies on the properties of the deposited sensing layer that defines the sensibility, selectivity and stability of the sensor response and depends on the choice of a suitable chemical environment towards the desired analytes [3]. While the hardware development has been already conveniently addressed and the state of the art of the oscillator circuits for such high frequency devices is today well established, the development of SAW sensor systems that intend be turned into real applications still relies on the properties of the sensing interface and, ultimately, in the choice of the sensitization material.

The sensing layer is achieved by the deposition of a suitable sensing material, which shall ideally show a selectivity towards the desired analytes in terms of the intermolecular

interactions based on the chemical environment provided by the sensing layer in the molecular level. In addition, the chemical and mechanical properties of the deposited sensing materials must also provide stability and reproducibility to the sensor's analytical response. The chemical and physical properties of the organic polymers as well as their diversity in terms of chemical constitution give rise to many applications of these kind of compounds at the molecular scale as drug transporters [4], support for catalysts [5], in the design of more specific and selective catalysts [6] and as sensitization layers of chemical sensors [7], among many others. Organic polymers have found a large use as sensing materials in chemical sensors due to the broad spectrum of molecular environments provided by the diversity of the chemical constitution of these macromolecules that can provide selective intermolecular interactions towards the chemical constitution of a given analyte [8–12]. Along with their large spectrum of chemical constitutions, the polymers also exhibit a large variety of structural properties, ranging from high crystallinity with their respective restrictions to the diffusion into its structure, to an amorphous, high porous, three-dimensional network, through which small molecules can easily access and diffuse [13]. For the sensitization of SAW sensors, besides the variety of possible structural chemical environments, the chemical and mechanical properties of polymers make them an excellent choice for the sensitization of complex surfaces [14], such as those of the SAW sensors elements once they fulfill the necessary requirements for a sensing layer to provide reliable SAW sensors [10,15–17].

The process of the production of a SAW sensor consists of the appropriate choice of the sensing material along with the suitable coating process to provide a coating layer over the surface of the piezoelectric substrate, which can operationally work with the electronics of the SAW sensor system. The choice of the coating process will therefore depend on the characteristic of the substrate and of the sensitization material used. Such deposition processes are also well established, and some of the used methods are electrospray, airbrush and spin coating [18,19]. The expected result in the production of a sensor is the deposition of the sensitization material, ideally forming a nanometric homogeneous layer that accounts for a minimal attenuation of the wave propagation and, at same time, possess a suitable composition and structure to absorb the quantities of the analytes necessary for their detection and quantification. The mass deposited on the sensitization layer, however, shall not overcome the limit that would stop the oscillation on the circuit. Finally, the sensing interface should be chemically and mechanically stable for a reasonable lifetime, expected for the utilization of the sensor system by real applications.

Therefore, the control and evaluation of the sensitization process are of great importance and shall make possible the characterization of the quality of the deposition. The control of the deposition starts by the measurement of the ultrasonic parameters: the frequency shift and the attenuation. Those integral parameters are used to determine whether the coated sensor will be operational on the sensor system. The deposition of the sensing material over the piezoelectric element is monitored by the measurement of the attenuation (S_{11}) and the resonance frequency shift before and after the material deposition. The attenuation measurement can be, to some extent, correlated with the homogeneity of the obtained layer and the material distribution over the sensing surface of the SAW piezoelectric element. The frequency shift, in turn, is related to the mass deposited over the sensitive area of the piezoelectric sensor element. These ultrasonic parameters are integral measurements and provide, therefore, an overall evaluation of the material deposition. A topological analysis of the deposition, especially over the active area of the piezoelectric substrate that could characterize the quality of the actual deposition in terms of its homogeneity and material distribution, shall be a very useful tool for the quality control of the process of sensor production as well as for the development of potential new sensing materials for SAW sensor technology.

In the previous parts of the work, we analyzed four chemically different polymers as sensing materials: polybutylmethacrylate (PBMA), polylaurylmethacrylate (PLMA), polyisobutylene (PIB) and Polychlorotrifluoroethylene co-vinylidene fluoride (PCTFE), and

their composites with Polyurethane (PU) as a new class of sensing materials [20,21]. The combination with PU to form composites showed a great improvement in the properties of the coating layer, as a high adhesion to the surface of the SAW sensor element, as well as improved chemical stability. In this part of the work, we make use of optical microscopy techniques associated with ultrasonic analysis to characterize the resulting coatings of the SAW sensor elements produced by the spin coating method using the above-mentioned pristine polymers and their respective PU-Polymer composites as the coating materials. To obtain an overview of the topological distribution of the material and to characterize the behavior of the layer deposited with the sensing materials over the complex surface of the piezoelectric sensor element, we used a combination of Dark Field Microscopy (DFM) and Bright Field Microscopy (BFM) [22,23]. The method allows the investigation of the sensing layer deposited over the SAW sensor element by a non-destructive direct measurement, and has the potential to be used as a tool for the evaluation of the coverage results obtained by the combination of new sensing materials and the used coating method.

The results of the optical microscopy together with the results of the ultrasonic operational parameters are used to investigate how far the actual aspects of the deposited layers, revealed by the microscopic methods, can be correlated to the integral ultrasonic measurements. The investigation of that correlation can significantly contribute to the development of new sensing materials as well as for the control of the quality of the coating process for the production of SAW sensors.

2. Methodology

2.1. SAW Sensor Elements

The surface of the SAW sensor element (purchased from SCD Components, Dresden, Germany) is made of a piezoelectric quartz substrate, having different regions where all structures are made of deposited lithographic gold (Figure 1). The larger dark rectangular structures in the four edges of the piezoelectric substrate are those used as electric contact pads. The region of the active area of the sensor are where the gold interdigital propagators for the acoustic waves are deposited in the form of tracks at the center, crossing the whole quartz substrate (dark grey structure). The light grey remaining regions around, as well as those forming a cross in the center of the piezoelectric element, are uncovered quartz substrate.

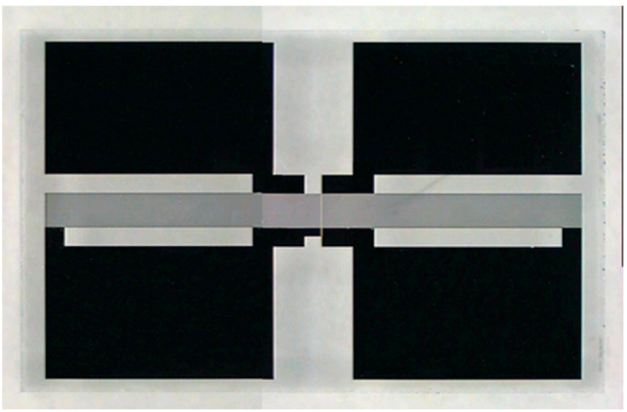

Figure 1. SAW sensor element (4 mm × 8 mm in size) with four large gold contact pads at the edges (in black color) and the active sensor area, containing the interdigital structure located in the center of the element (the continuous dark gray zone that crosses horizontally the whole element). The horizontal and vertical light gray remaining regions are the quartz substrate parts, which are free of any gold deposition.

2.2. Spin Coating Procedure

The pristine polymers were dissolved in THF at a concentration of 50 mg.mL^{-1}. Then, 100 µL of these original polymer solutions were diluted with 1400 µL of THF to form their

respective spin coating solutions for the deposition, as described below. For the pristine PU, 200 µL of a PU solution (15 mg·mL^{-1}) were diluted with 1300 µL of THF to form its spin coating solution. For the PU-Polymer composites, 100 µL of the original polymer solutions (50 mg·mL^{-1}) were mixed with 200 µL of the PU solution (15 mg·mL^{-1}), and then 1200 µL of THF were added to form the PU-Polymer composite spin coating solutions. All the concentrations were chosen to enable the production of operational SAW sensors.

For the coating, 200 µL of the respective spin coating solutions of each coating material were dropped over the piezoelectric sensor element placed on the spin coater (Laurell MS-400B-6NPP/LITE, Lansdale, PA, USA). The rate of rotation speed used was 8000 rpm for 120 s. All parameters were precisely controlled. With this procedure, the concentrations of all polymers were the same in the spin coating solutions. The concentration of PU was also maintained constant in all the composite spin coating solutions.

2.3. Ultrasonic Parameters

The SAW sensors elements were tested before and after depositions using a Network Analyzer (Hewlett Packard 8712ES, Waldbronn, Germany) to obtain the ultrasonic parameters, frequency shift, and the acoustic attenuation (S_{11} parameter).

2.4. Bright- and Dark Field Microscopy (BFM/DFM)

The microscope Axiotech 100 HD (Carl Zeiss, Jena, Germany) was used in the analyses of the coated surface of the SAW piezoelectric element. The object of interest is the active area of the sensor in the central part of the piezoelectric sensor element (Figure 1). Different magnifications and both techniques of DFM and BFM were used in the analysis to provide a better visualization of the depositions.

2.5. Chemicals

Tetrahydrofurane (CAS 109-99-9) was purchased from Sigma-Aldrich Co. (St. Louis, MO, USA); PBMA (CAS 9003-63-8), PLMA (CAS 25719-52-2), PIB (CAS 9003-27-4) and PCTFE (CAS 9010-75-7) were purchased from Sigma-Aldrich Co. (St. Louis, MO, USA). The polyurethane (polymeric methylenediphenyldiisocianate and polyether-polyester basis) was obtained from Büfa Company, Oldenburg, Germany. All the polymers and the solvent were used without further purification.

3. Results and Discussion

In this work, the characterization of the quality of the deposition of the coating process and of the resulting coating layer for the SAW sensor technology is done by considering two main aspects. The first aspect is the uniformity of the material distribution, and the second one is the homogeneity of the resulting coating layer. Both aspects depend mainly on the coating method and on the properties of the coating material and its respective interaction with the surface of the SAW sensor element.

To exemplify the problems that can affect each aspect on the result of the coating process, a bad material distribution can arise from a quick modification of the viscosity by the evaporation of the solvent during the spinning step of the coating, which can be intensified by the specific affinity between the coating material with the different regions of the SAW sensor element that could lead to different concentrations of material over the surface of the sensor element.

A lack of homogeneity can arise from differences in the interaction of the isomers of the polymer with the regions of the SAW sensor element, which could lead to a gradient of concentration of the constituents of the polymer, resulting in locally distinct profiles of specific gravity. In the case of composites, the same can occur, and even more significantly due to a possible separation of their components during the spin coating, also creating a local gradient—in this case, of different materials.

Scheme 1 illustrates how the quality of the material distribution and the homogeneity of the resulting coating layer can vary. The typical structural results of the coating process are pictorially represented by the four regions of the graphic in Scheme 1.

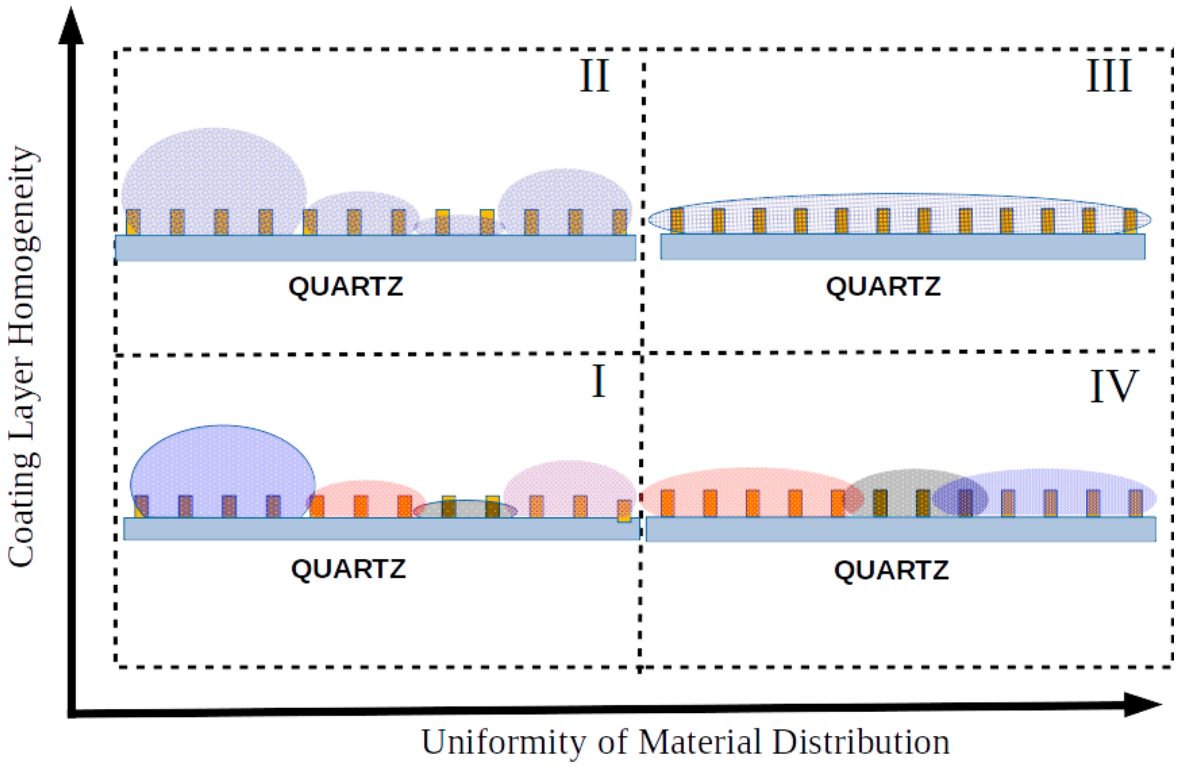

Scheme 1. Aspects of the structural results of the coating process and their typical variations, illustrated by the four regions in the graphic. The surface of the active area of the SAW sensor element is represented by the quartz substrate and the gold electrodes (yellow rectangles over the quartz substrate). Region I: bad material distribution and low homogeneity of the deposition, represented by the different colors of the deposition in the figure. Region II: bad material distribution and high homogeneity of the deposition. Region III: good material distribution and high homogeneity of the deposition. Region IV: good material distribution and low homogeneity of the deposition, represented by the different colors of the deposition in the figure.

Based on those definitions, the results of the optical microscopy of the coating layers obtained for each pristine sensing polymer as well as for their composites with PU are analyzed and correlated with the results of the ultrasonic parameters (Section 2.3).

3.1. Ultrasonic Analysis

The ultrasonic results of the attenuation and of the frequency shift obtained for the pristine polymers are shown in Tables 1 and 2, which present the results obtained for the PU-composites with each sensing polymer.

Table 1. Ultrasonic results for the coating obtained with the four pristine sensing polymers.

Pristine Polymer	Frequency Shift/MHz	Attenuation/dB
PU_200	0.15	4.75
PBMA_100	0.14	5.35
PLMA_100	0.73	8.59
PIB_100	0.45	6.27
PCTFE_100	1.49	8.36

Table 2. Ultrasonic results for the coating obtained for the composites of the sensing polymers with PU.

Polymer Composite	Frequency Shift/MHz	Attenuation/dB
PU_200_PBMA_100	0.66	8.95
PU_200_PLMA_100	1.98	13.89
PU_200_PIB_100	1.27	10.95
PU_200_PCTFE_100	1.61	7.23

Considering the results shown in Tables 1 and 2 and the fact that all the polymers are in the same concentration, the variations presented by the results of ultrasonic measurements can be interpreted as the result of the interaction of each polymer with the surface of the SAW sensor element through the spin coating process. This is a complex mechanism involving the physicochemical properties of the polymers and their interaction with the complex surface of the SAW sensor element, occurring as the solvent evaporates during the coating processing.

The resulting mass over the active area of the sensor can be indirectly inferred by the frequency shift measurement. As is well known, the frequency shift measurement is affected by the viscoelastic properties of the polymeric coating, which depends on the chemical constitution and resulting structure of the polymeric layer. Despite the complexity of the process, the value of the frequency shift allows a practical inference about the actual deposited mass of the coating layer over the active area of the sensor, which accounts for the sensor performance.

Figure 2 summarizes the frequency shift values obtained for the coatings with the pristine polymers and their corresponding PU-composites.

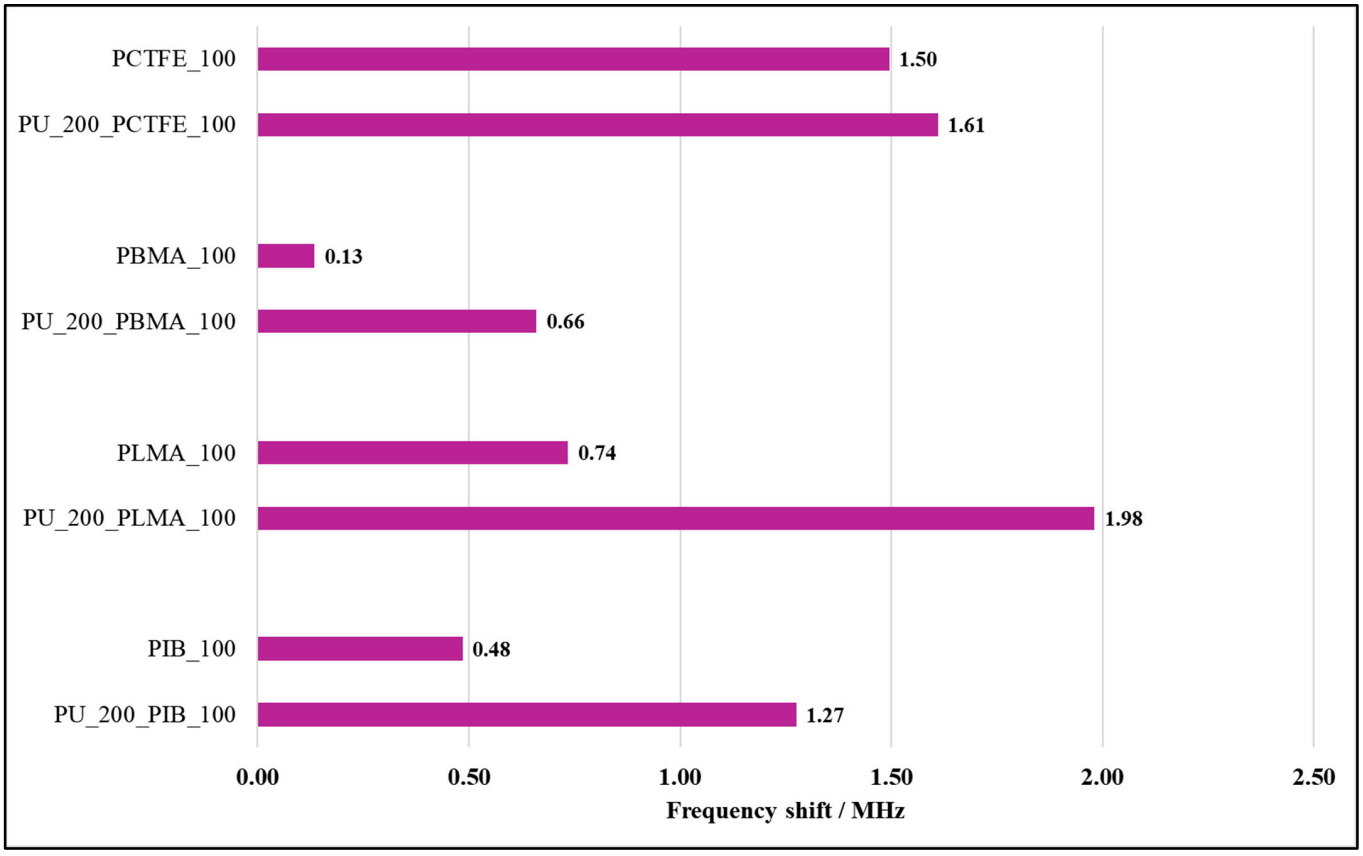

Figure 2. Frequency shift results of the pristine sensing polymers and their PU-composites.

The increase in the frequency shift observed in the PU-composites in comparison to the pristine polymer is expected because of the increase of the polymer concentration in the coating solution as well as due to the incorporation of more sensing polymers in the coating layer by the combination with PU, as demonstrated in the previous work [21].

Regarding the pristine polymers, the PCTFE was the only polymer to which the frequency shift before and after the combination with PU did not present such a significant difference like those observed by the other pristine sensing polymers. A possible explanation for this observation lies in the more distinguished chemical constitution of PCTFE from the other polymers, which can consequently lead to distinguished interactions with the SAW sensor surface as well as to form a quite distinct composite with PU, as was observed in the previous work [21].

Figure 3 shows the measured values of the attenuation for the tested polymeric coating materials.

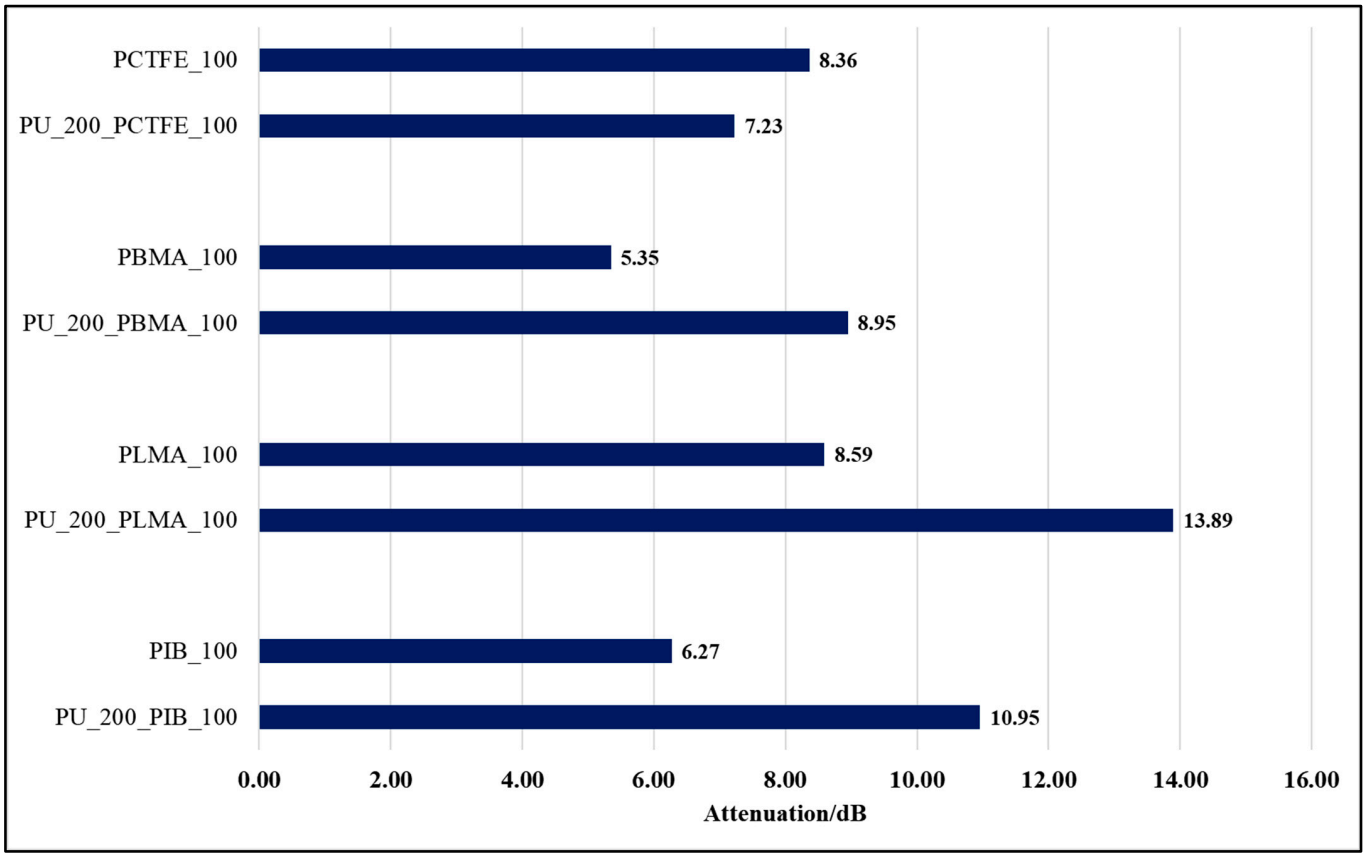

Figure 3. Attenuation results of the pristine sensing polymers and their PU-composites.

The attenuation can be interpreted as the resistance offered by the coating layer to the wave propagation (due to energy dissipation) over the surface of the SAW sensor element, and is the parameter whose value determines in the practice whether a coated sensor will work or not on the oscillator circuit of the SAW system. In the case of coating layers of polymers, the attenuation shall depend on factors like chemical constitution, nature and structure of the polymer network, crystallinity, and viscoelastic properties of the resulting polymeric layer, among others.

Aside from intrinsic chemical and structural factors, in terms of the resulting coating layers obtained by the coating process used, the value of the attenuation shall also depend on the quantity of material deposited, on the uniformity of the material distribution over the active area of the SAW sensor element, and on the homogeneity of the sensing layer itself, especially in the case of composite materials. In general, the increase of the mass deposited as well as the lack of uniformity of the material distribution by the coating

process and the inhomogeneity of the deposited layer itself will account for an increase in the attenuation values.

The values of attenuation for the deposition with the pristine polymers (Figure 3) shows an increasing scale, where the PBMA presented the lowest value of attenuation, followed by PIB, and the highest values were found for PLMA and PCTFE, which presented very close values of attenuation. The values reflect the properties of the coating layer of each polymer as a result of the coating method and experimental conditions.

The attenuation values for the PU-composites with PLMA, PBMA and PIB agree with the results obtained for the pristine polymer coating layers, showing the consequent increase in the attenuation expected solely by the increase of the deposited mass, which can also be observed by the results of frequency shift (Figure 2). The increase of values of attenuation for the PU-Polymer composites follow the same order observed for the pristine polymers. The exception is the behavior of PCTFE, where the attenuation of its PU-composite was lower than that observed for the pristine polymer (Figure 3). As discussed for the frequency shift measurement, this odd behavior relies on the quite distinct chemical composition of PCTFE in comparison to the other polymers investigated, which shall lead to the formation of a corresponding distinct PU-composite.

As observed in the previous work [21], the formation of the PU-composites seems to follow a similar mechanism. Accordingly, the new PU-composites prepared in this work shall also share similarities in their mechanisms of formation, and this fact was verified by the obtained ultrasonic results.

In the attempt to identify the correlation between the pristine polymer coating layers and those formed by their respective PU-polymer coating layers, Figure 4 presents the graphic of the frequency shift values measured for the PU-polymer composites against the frequency shift values obtained for the corresponding pristine polymers.

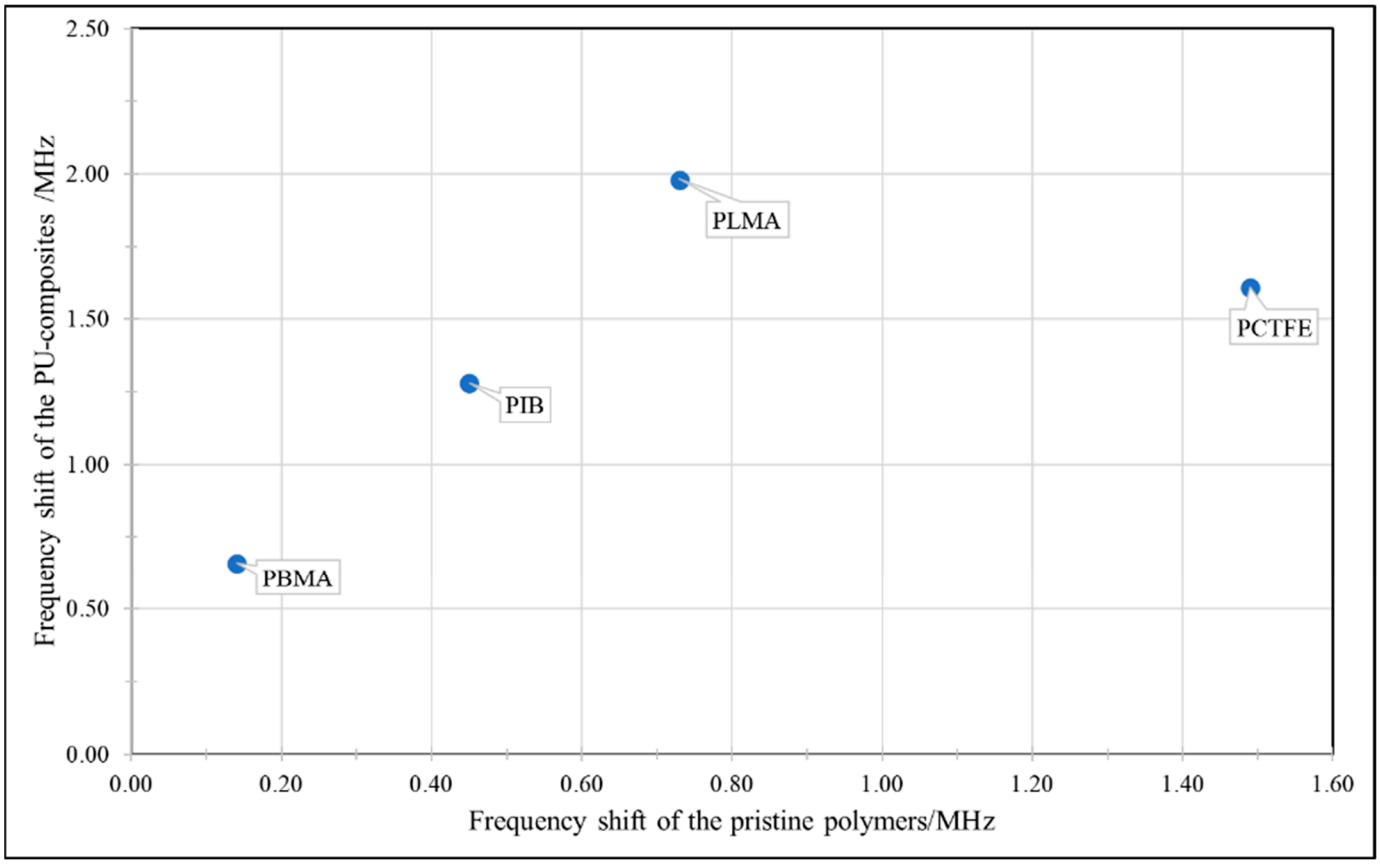

Figure 4. Frequency shift of the PU-Polymer composites vs. the frequency shift of the respective pristine sensing polymer.

As can be seen in Figure 4, the PCTFE result shows a significant deviation from the behavior observed by the other polymers. By removing the data of PCTFE, the results of the frequency shift for the PU-polymer composites show a good correlation with the results of their respective pristine polymers (Figure 5). This kind of correlation was intensively explored in the previous work [21], and it again emerges from the ultrasonic data for the polymers and their respective PU-composites formed using the methodology developed in the work. Here, it must be considered that the PU-polymer composites used in this work are different from those used in the previous work.

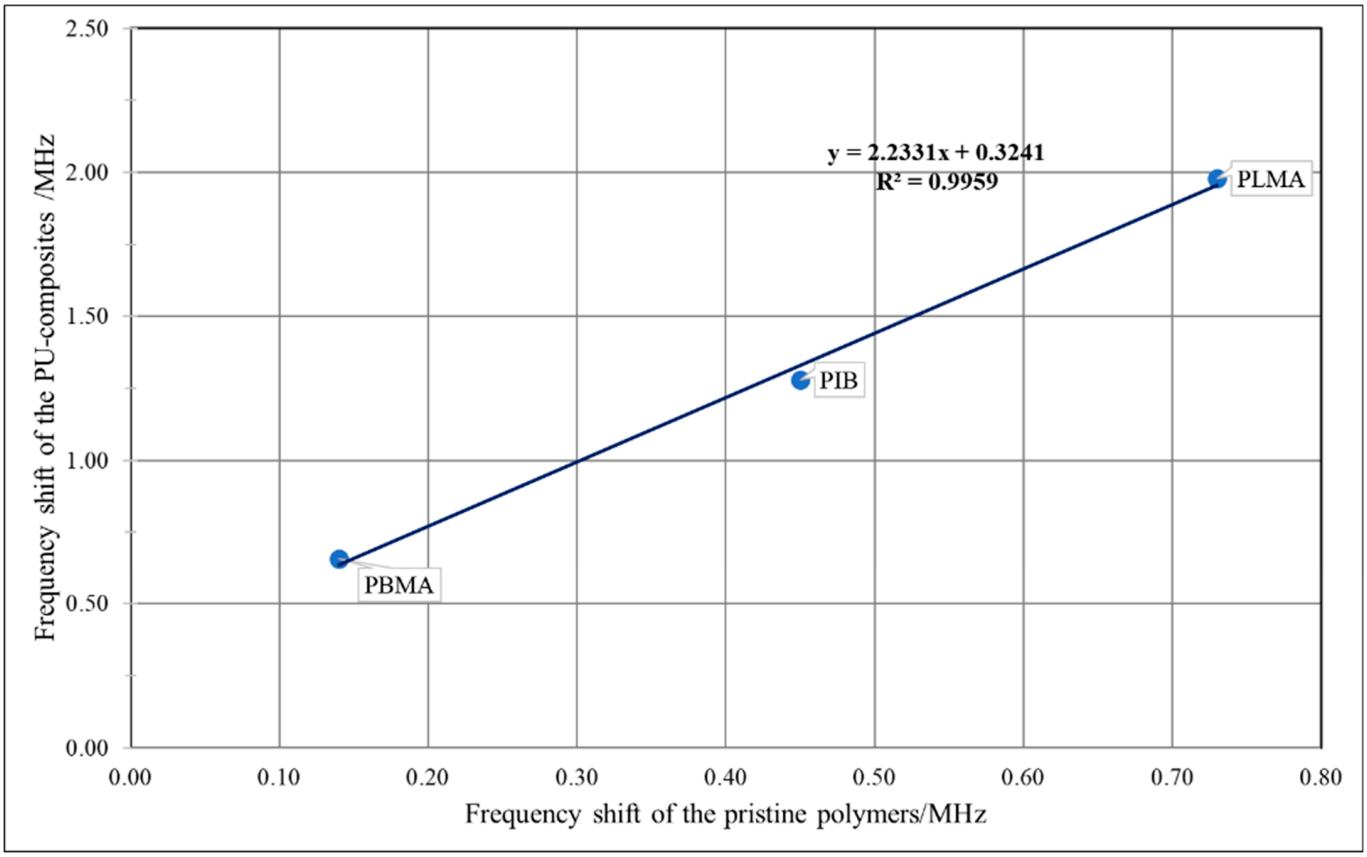

Figure 5. Correlation of the frequency shift of the PU-Polymer composites vs. the frequency shift of the respective pristine sensing polymer (excluding the PCTFE data).

In the same sense, the analysis of the results of attenuation also indicates the observed correlation between the coating layers obtained with the pristine polymers and those with their respective PU-polymer composites.

This also indicates that the formation of the PU-PCTFE composite is quite distinct from that experienced by the other polymers. Figure 6 presents the graphic of the attenuation results for the PU-polymer composites against the attenuation values obtained for their respective pristine polymers. The same behavior observed for the frequency shift is reproduced by the attenuation results. Again, the off-scale value belongs to PCTFE, reinforcing the supposition about the distinct behavior of this polymer as coating material either in the pristine form as well as in the form of its PU composite.

By removing the PCTFE data, the attenuation values also show a good correlation between the results for the PU-composites and their respective forming pristine polymers (Figure 7).

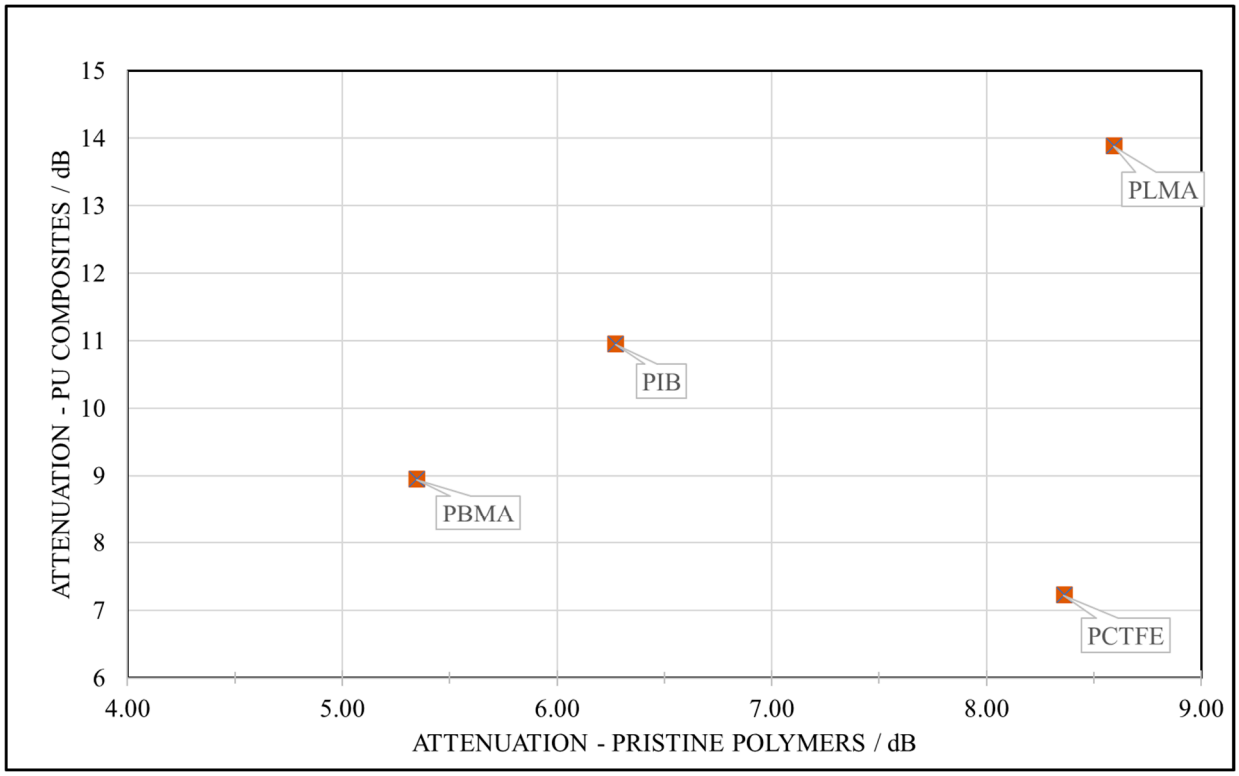

Figure 6. Attenuation of the PU–polymer composites vs. the attenuation values of the respective pristine sensing polymer.

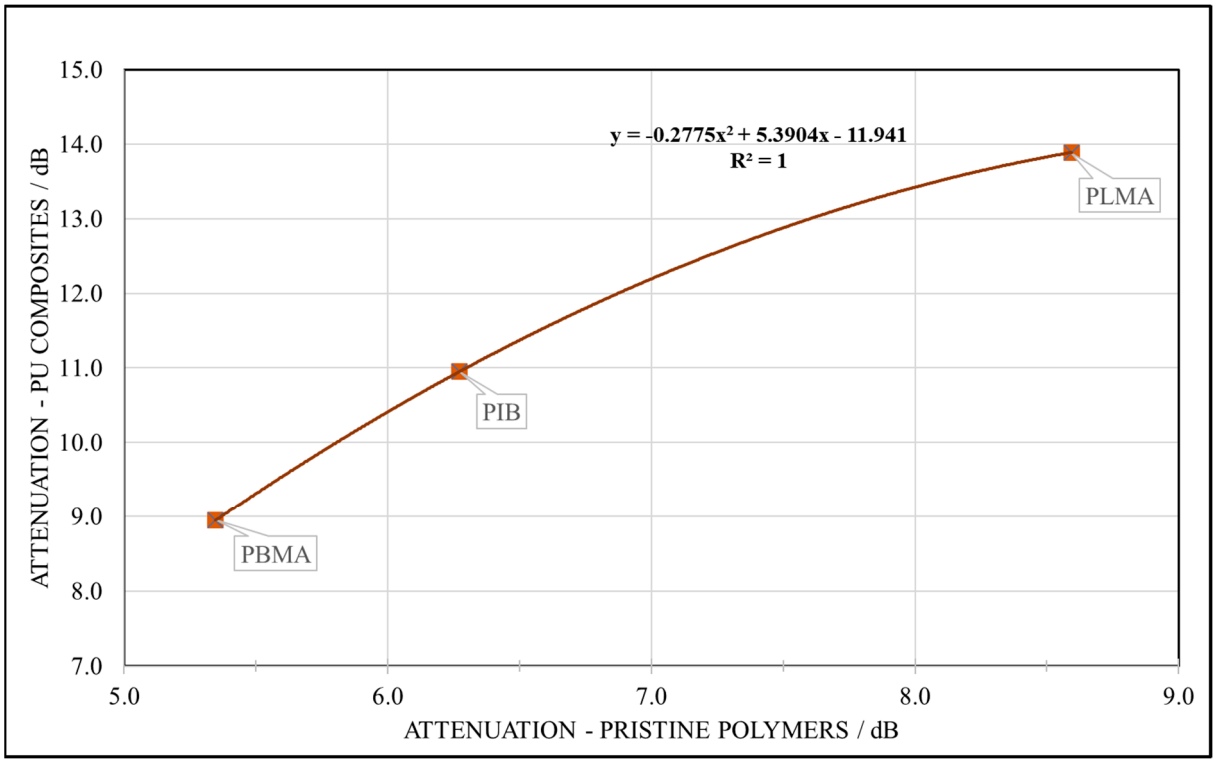

Figure 7. Correlation between the attenuation of the PU–polymer composites vs. the attenuation values of the respective pristine sensing polymer (excluding the PCTFE data).

The numerical correlations for the ultrasonic parameters observed between the PU–polymer composites and their respective forming polymers indicate that, even though the

coating layers formed by the combination with PU show distinct properties, due to the chemical differences between the respective forming polymers, they seem to be formed by a similar mechanism.

For a more complete evaluation of the performance of the coating layers and of the coating process itself, it is important to access information of the actual material distribution and the homogeneity of the coating layers, especially when one is dealing with composite materials.

In the ultrasonic analysis, the attenuation is the parameter that could be correlated to the material distribution and its homogeneity, even considering that the ultrasonic attenuation has an integral aspect reflecting an "averaged" value in this way; that is correlated to the actual quality of the material distribution and to differences in the homogeneity of the coating result.

To use the attenuation values for a correlation with the coating results, the influence of the material quantity of the deposited coating layer is isolated from the analysis once it contributes significantly to the attenuation results. One way to do this is to express the attenuation pro unity of frequency shift for a given coating layer, since the frequency shift is correlated to the mass deposited over the active area of the sensor element. The quotient of the attenuation by the frequency shift (QAF) for a given coating can express a "specific attenuation", the values of which are interpreted as the influence of the material properties on the observed attenuation, independently of the contribution of the mass of the coating to the attenuation results.

Figure 8a presents the results of the QAF for all the pristine polymers and the pristine PU coating, and Figure 8b presents their respective PU-composites. The calculation was made using the data from Tables 1 and 2.

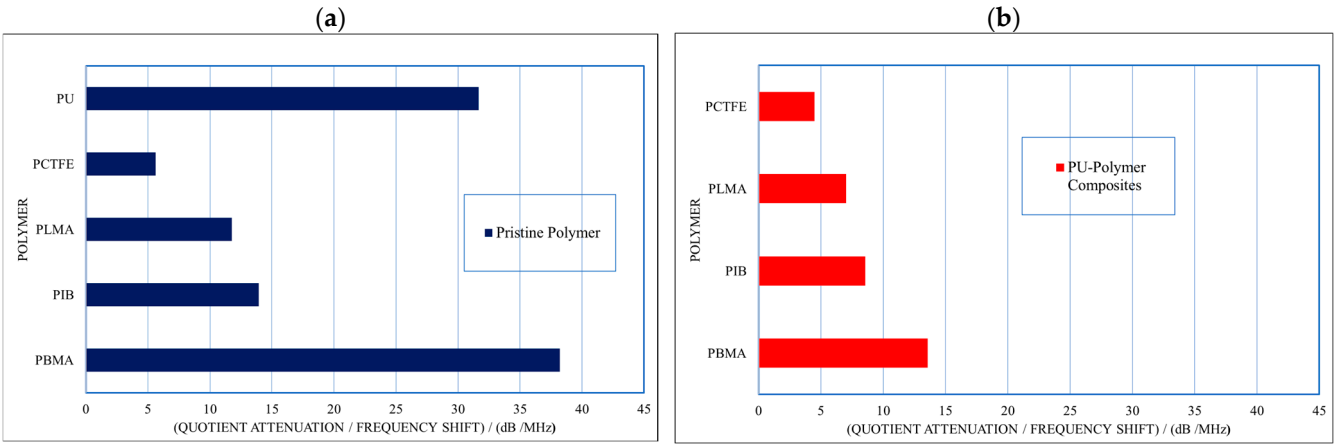

Figure 8. Results of the QAF for (**a**) all the pristine polymers and the pristine PU coating and (**b**) their respective PU-composites, calculated using the data from Tables 1 and 2.

The QAF results lead to new information about the coating layers. The first observation is that the values of the QAF for the pristine polymers follows the same order observed for the original values of attenuation (Figure 3), but in an inverse way. A lower value of attenuation corresponds to a higher value of the QAF, maintaining the sequence observed for the increase of the attenuation values. The value for the pristine PU coating agrees with the microscopy observations, as will be further discussed. The same behavior is observed for all the PU-polymer composites, exactly reproducing the inverse that was observed for the original attenuation results (Figure 3). Therefore, the values of the QAF can be associated with the enhancement of the propagation of the acoustic wave over the surface of the SAW sensor element. The results suggest that the higher the values of the QAF, the lower the resistance to the acoustic wave propagation over the surface. Considering that the QAF results are independent of the mass of the depositions, the difference between them relies on the properties of the actual coating deposition: its chemical composition,

its uniformity, and its homogeneity. Therefore, the results of QAF shall be useful in the interpretation of structural analysis of coating results.

The differences between the coating materials are inherent to their chemical constitutions. Therefore, the QAF values for each pristine polymer are expected to be different from each other. The values for the PU-composites are quite distinct from those of their respective pristine polymer since the PU-polymer composites are chemically totally distinct from their forming polymers. Therefore, the general decrease of the QAF observed for the PU-composites when compared to their forming pristine polymer relies on the chemical constitution of the composites and their respective intrinsic properties. More investigation must be made to find out whose properties can be associated with the attenuation mechanism operating in the process.

As was made for the original values of attenuation (Figure 7), the analysis of the QAF values for the pristine polymer and those for their respective PU-polymer composites also show a very good correlation between the data (Figure 9).

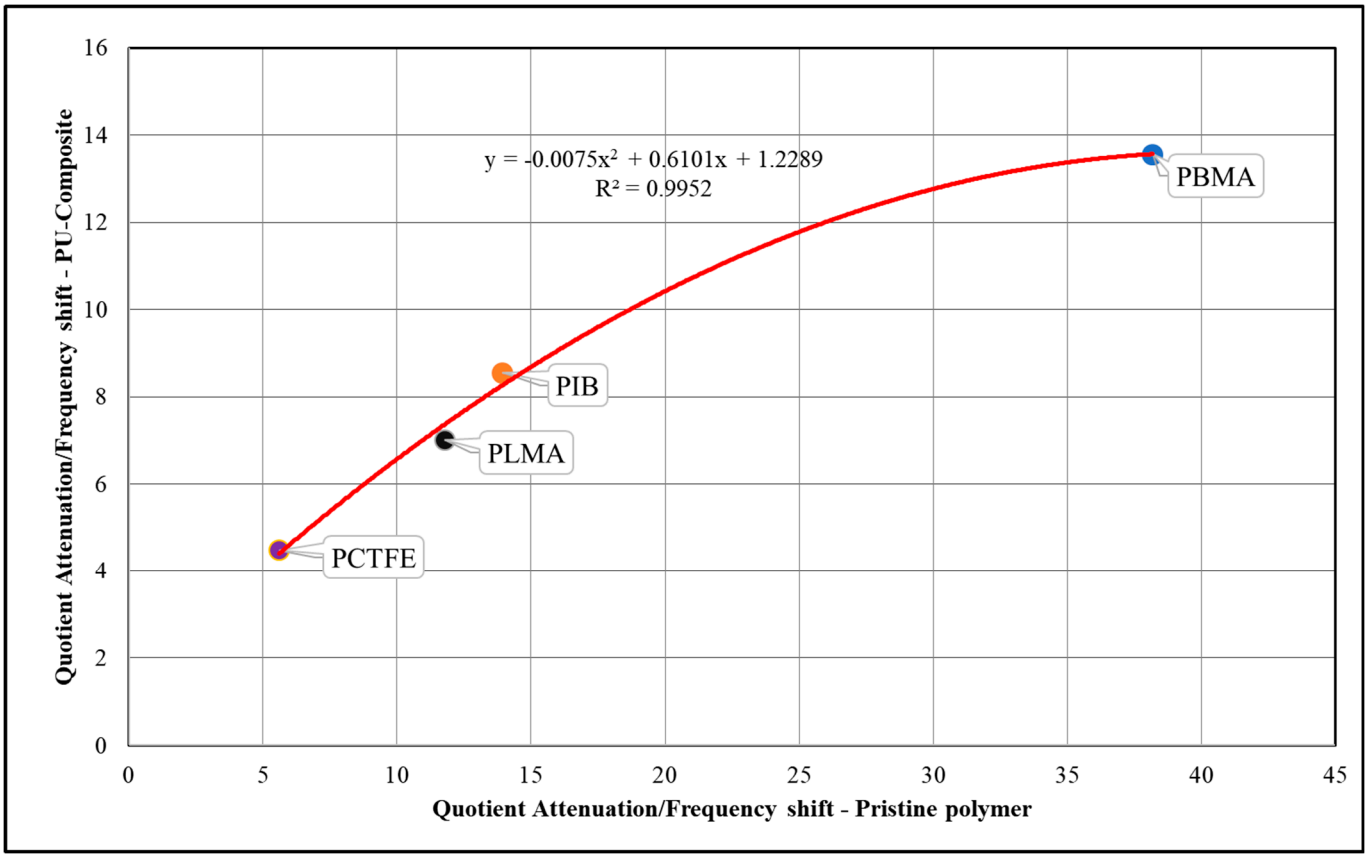

Figure 9. Correlation between the QAF of the pristine polymers and the QAF of their respective PU-composites.

Taking in account the QAF results, the correlation also includes the PCTFE in the relationship found for the coating materials, which is a good indication that the concept of a specific attenuation can better describe the behavior of chemically distinct coating materials.

The good correlation between the QAF data (Figure 9) reinforces the supposition that although all the PU-polymer composites are distinctly constituted, they are formed through a similar mechanism.

After the analysis of the ultrasonic results, it is important to correlate all the results obtained by the ultrasonic analysis to the actual structure of the coating layers to see how much the results of the ultrasonic parameters can be related to the results of the depositions obtained by the used coating method.

3.2. Dark and Bright-Field Microscopy

The BFM and DFM observations are now presented. The microscopic methods are alternately used to get the best visualization of the coating results. The observations in the ultrasonic analysis will be correlated to the BFM and DFM results.

3.3. PU Sensing Layer

Figure 10 presents the exposures for the resulting coverage with pristine PU as the coating material.

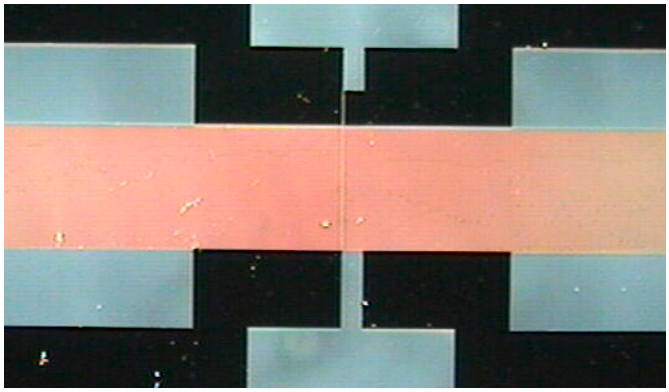

(**a**)

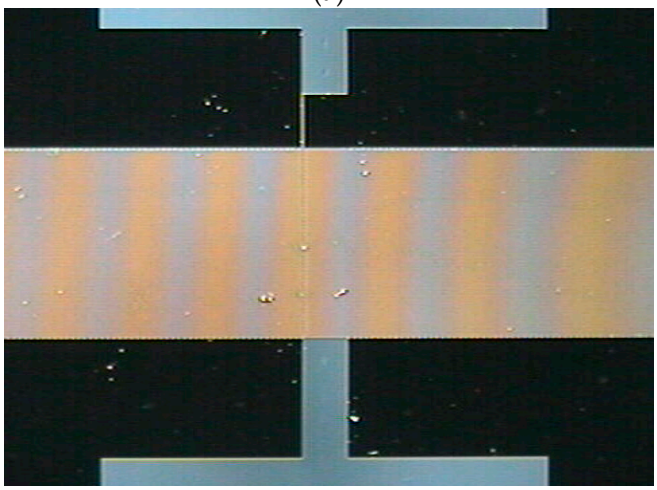

(**b**)

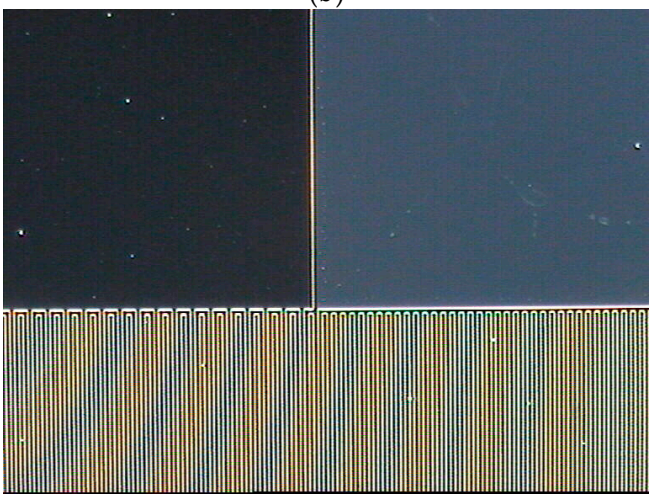

(**c**)

Figure 10. *Cont.*

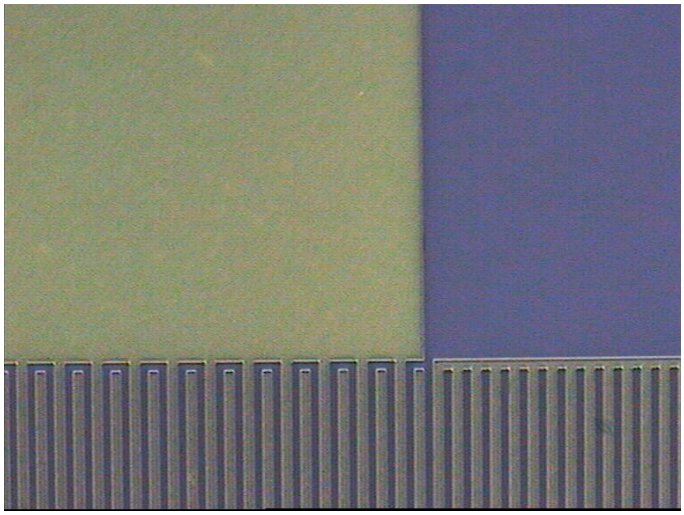

(**d**)

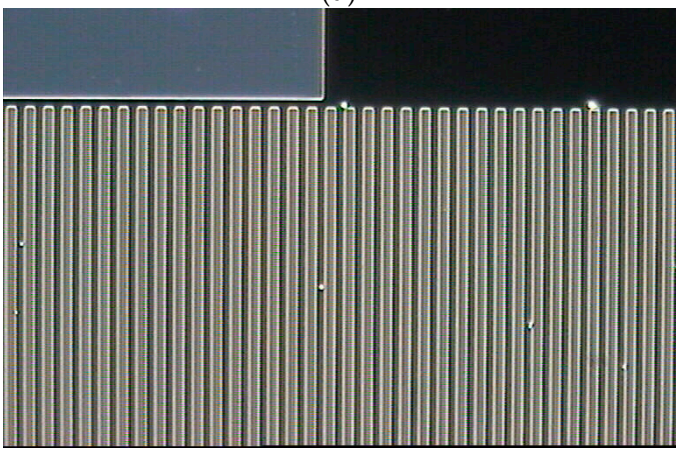

(**e**)

Figure 10. BFM/DFM exposures of the pristine PU sensing layer. The coating results show good homogeneity and uniformity of material distribution. (**a**) Magnification 5× with DFM. (**b**) Magnification 10× with DFM. (**c**) Magnification 50× with BFM. (**d**) Magnification 100× with DFM. (**e**) Magnification 100× with BFM.

For the sensing layer of pristine PU, the DFM 5- and 10-times magnifications (Figure 10a,b) show a relatively good uniformity of material coverage with this polymer. Sparse particles can be seen over the whole area of the sensor element. In the BFM 50-times magnification exposure (Figure 10c), the uniformity of the material distribution over the interdigital structure (active area of the sensor) can be clearly seen, as well as the homogeneity of the coating layer. In the 100-times magnification, by both DFM and BFM exposures (Figure 10d,e), the homogeneity of the pristine PU coating layer can also be observed, especially in the sensor's active area.

This fact agrees with the ultrasonic results, as the coating layer of pristine PU polymer showed the lowest attenuation within the pristine polymers (Table 1), suggesting a high homogeneous deposition. The microscopy results (Figure 10) suggest a good interaction with all kinds of the surfaces, especially with the interdigital structure, the active area of the SAW sensor element.

3.4. PBMA Sensing Layer

Figure 11 presents the images for the deposition of pristine PBMA as sensing material.

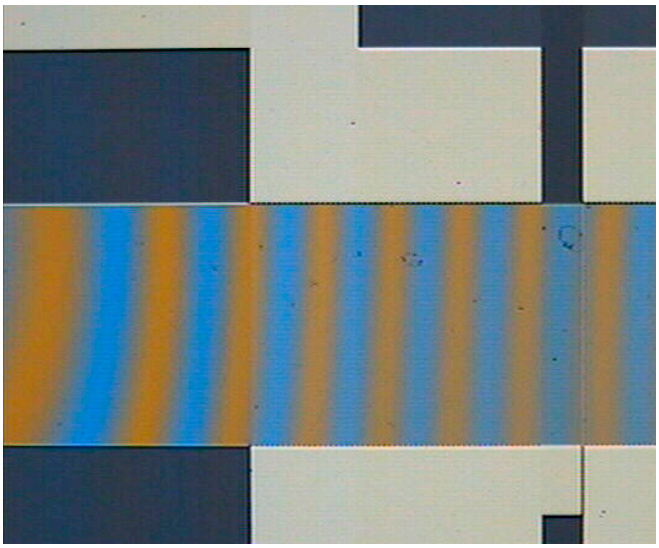

(**a**)

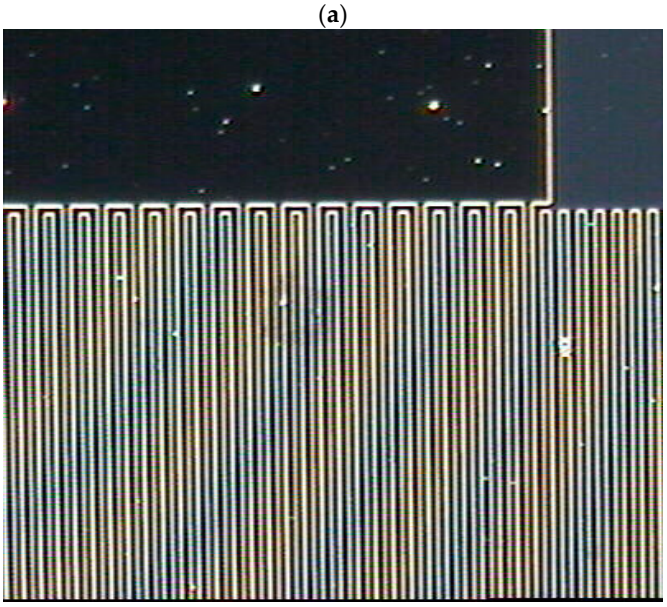

(**b**)

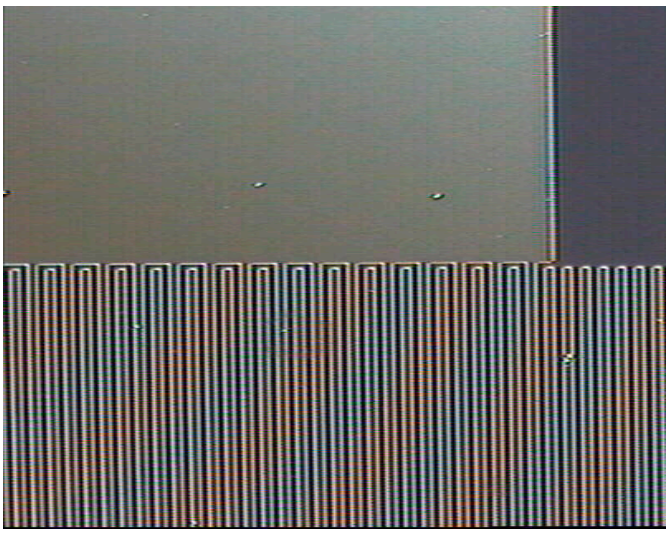

(**c**)

Figure 11. *Cont.*

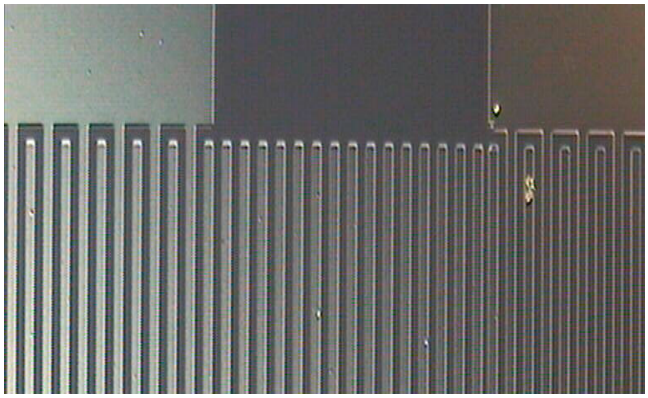

(**d**)

Figure 11. Exposures of the pristine PBMA sensing layer. The coating presented a good overall uniformity of material distribution, and the layer shows also good homogeneity. (**a**) Magnification 10× with DFM. (**b**) Magnification 50× with BFM. (**c**) Magnification 50× with DFM. (**d**) Magnification 100× with DFM.

The DFM exposure of 10-times magnification indicates a high degree of uniformity in the pristine PBMA coating layer (Figure 11a). The BFM exposure of 50-times magnification (Figure 11b), as well as the DFM exposure with the same magnification (Figure 11c), shows the same aspect of an overall uniform material distribution along the active sensor area as also indicates the homogeneity of the pristine PBMA deposition. The DFM 100-times magnification (Figure 11d) also indicates homogeneity and a uniform material distribution over all the different regions of the piezoelectric element. These observations agree with the ultrasonic result of the attenuation for the pristine PBMA coating layer. The attenuation value of the PBMA coating layer is the second lowest between all the pristine polymers' depositions (Table 1).

These results indicate that both polymers PU and PBMA may have a good interaction with all the structures of the different regions of the surface of the SAW sensor element, indicating a uniform and homogeneous coverage of the active sensor area.

3.5. PU-PBMA Composite Sensing Layer

Figure 12 presents the exposures for DFM and BFM of the PU-PBMA composite deposited as the sensing layer.

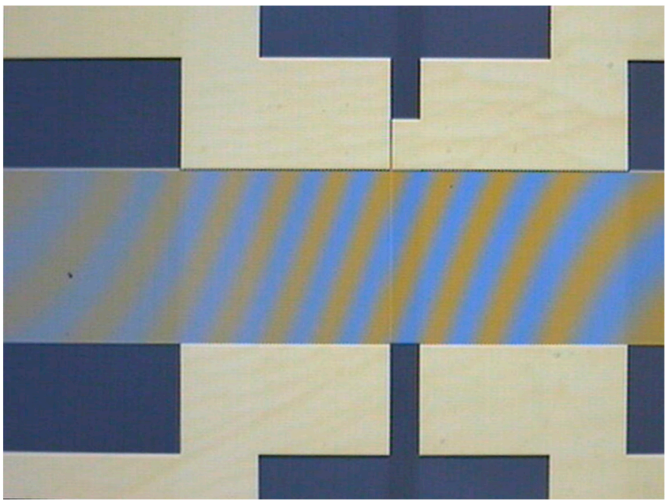

(**a**)

Figure 12. *Cont.*

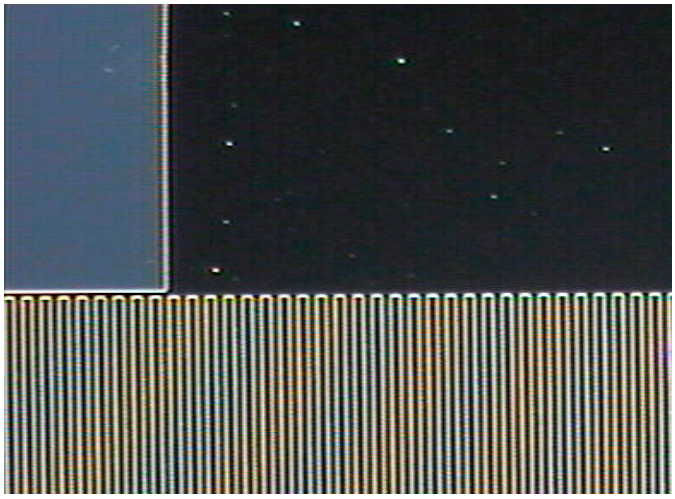

(**b**)

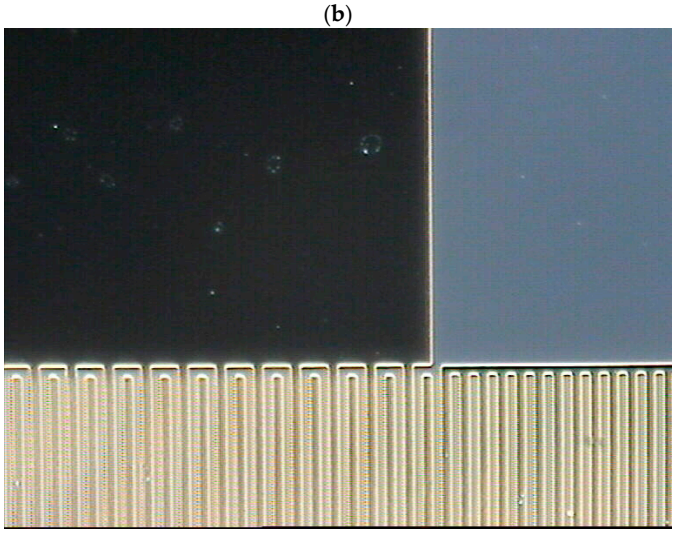

(**c**)

Figure 12. Exposures with both BFM and DFM of the PU-PBMA composite deposited as the sensing layer. The composite presented the same good results as its individual former polymers did: good homogeneity and good material distribution. (**a**) Magnification 10× with DFM. (**b**) Magnification 50× with BFM. (**c**) Magnification 100× with DFM.

As can be seen in Figure 12, the exposures of the coated SAW sensor element with the PU-PBMA composite as the sensing layer presented the same quality of deposition in terms of uniformity and homogeneity of the deposited sensing layer, as observed for the pristine PBMA coating layer shown in Figure 11.

3.6. PLMA Sensing Layer

For the deposition of pristine PLMA as the sensing material, the exposures for DFM and BFM are presented in Figure 13.

The exposures of the deposition with pristine PLMA as the sensing material (Figure 13) show quite different results of material distribution from those observed for PBMA and PU. From exposures of 10-times magnification, by both BFM and DFM, the poor uniformity of the material distribution over the whole area of the SAW sensor element can be seen (Figure 13a,b). The exposures of 50-times magnification show different distributions of the pristine PLMA coating polymer over the three different regions of the surface of the SAW sensor element.

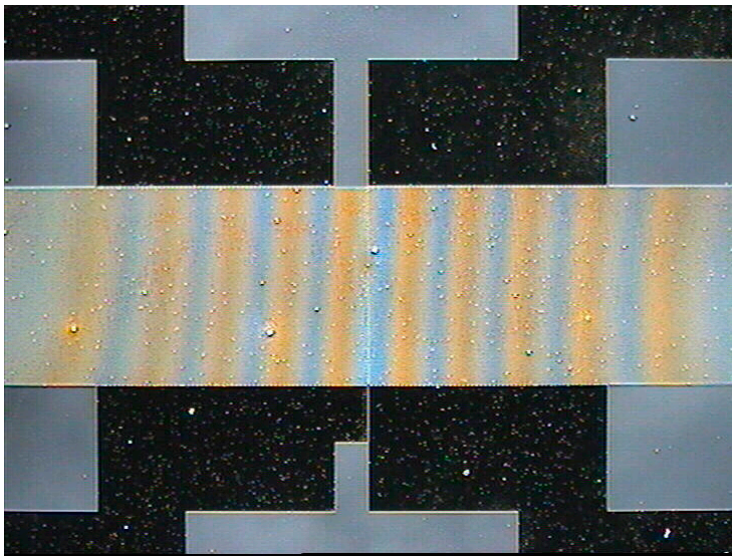

(**a**)

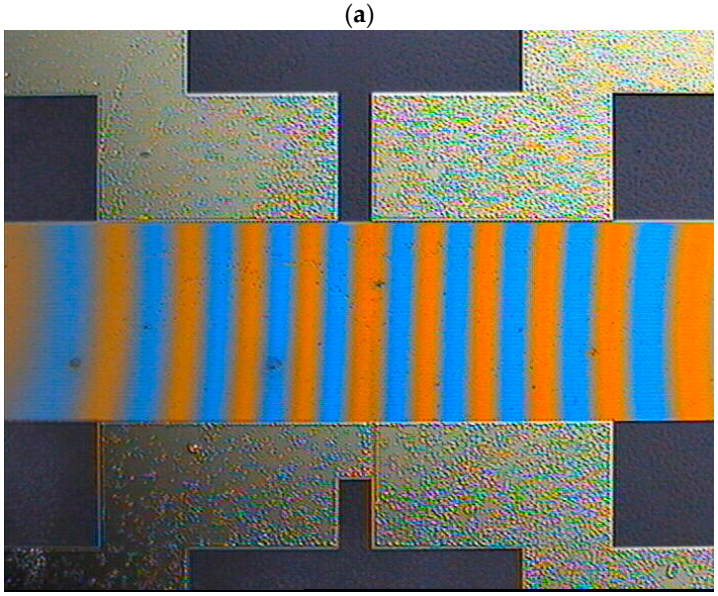

(**b**)

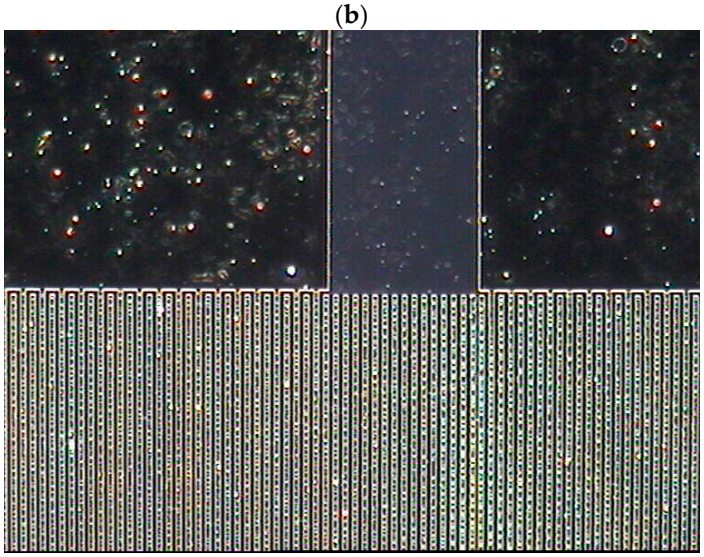

(**c**)

Figure 13. *Cont.*

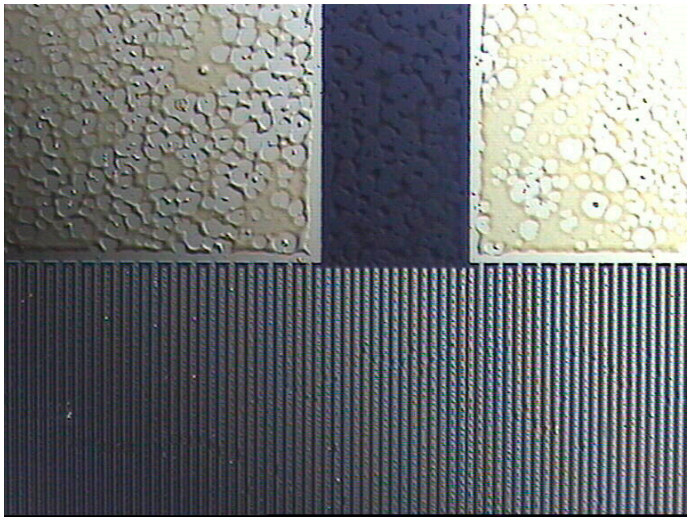

(**d**)

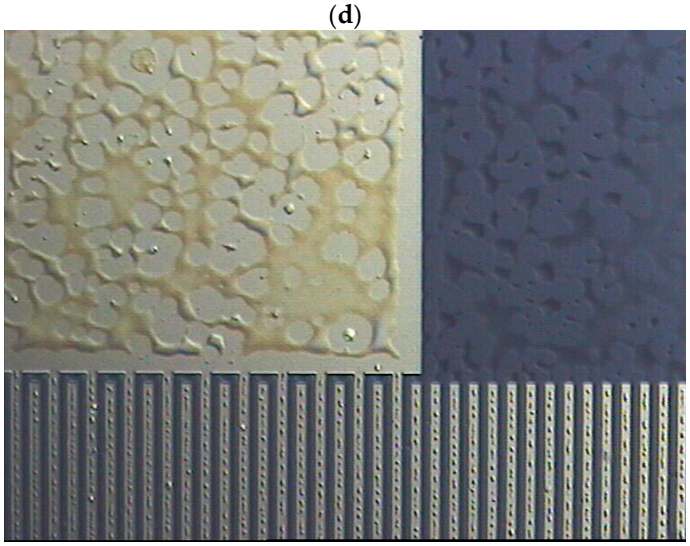

(**e**)

Figure 13. Images of the deposition of PLMA as sensing nanometric layer. The coating results for the pristine PLMA showed a poor material distribution throughout the sensor element regions. (**a**) Magnification 10× with BFM. (**b**) Magnification 10× with DFM. (**c**) Magnification 50× with BFM. (**d**) Magnification 50× with DFM. (**e**) Magnification 100× with DFM.

Over the large gold pads (large yellow parts above the interdigital structure in Figure 13d), it can be seen that the deposited material does not become wet significantly on the gold surface, which indicates the poor adhesion of the coating. The inspection of the active sensor area in more detail can be done by the DFM exposure of 100-times magnification (Figure 13e), where the coating material is seen in the form of small droplets all over the top of the gold fingers of the interdigital structure of the active sensor area, and the presence of coating material can also be noted in between the gold fingers, where the surface is quartz.

These observations are supported by the ultrasonic results for the PLMA deposition. The frequency shift value for the deposition of pristine PLMA presented the second highest value between the depositions with the pristine polymers, indicating one of the highest deposited masses obtained by the depositions with the pristine polymers (Figure 2). The value of the attenuation was, however, the highest obtained by the pristine polymer coating layers (Figure 3), which is caused by the poor material distribution shown by the microscopy results.

A possible explanation for the distinct behavior observed for the pristine PBMA and PLMA depositions can be found by comparing their chemical structures. Though both are polyacrylate polymers, the main structural difference between them is their side chains, which are a butyl group in the case of PBMA and a lauryl group in the case of PLMA. Being a large linear hydrocarbon chain, the lauryl group increases the aliphatic character of PLMA in comparison to PBMA, which leads to the poorer interaction observed with the quartz-metallic substrates of the SAW sensor element surface. Even a small variation of the number of carbon atoms in the structure of organic molecules can significantly influence their properties as well as the properties of their polymers and composites [24].

3.7. PU-PLMA Composite Sensing Layer

Figure 14 presents the exposures for DFM and BFM of the PU-PLMA composite deposited as the sensing layer.

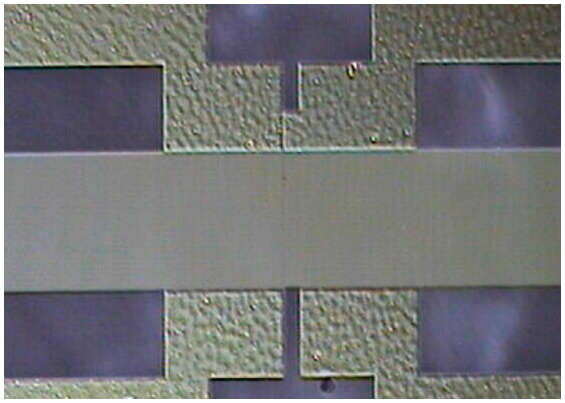

(**a**)

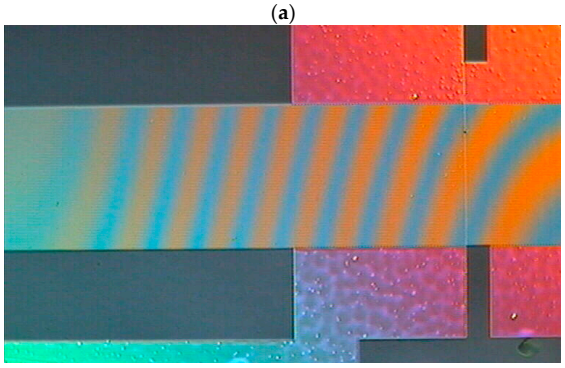

(**b**)

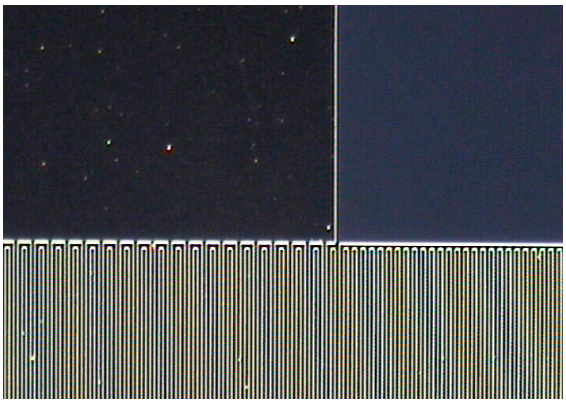

(**c**)

Figure 14. *Cont.*

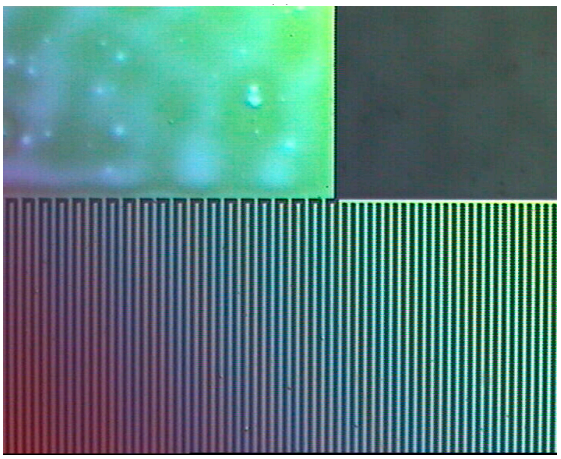

(**d**)

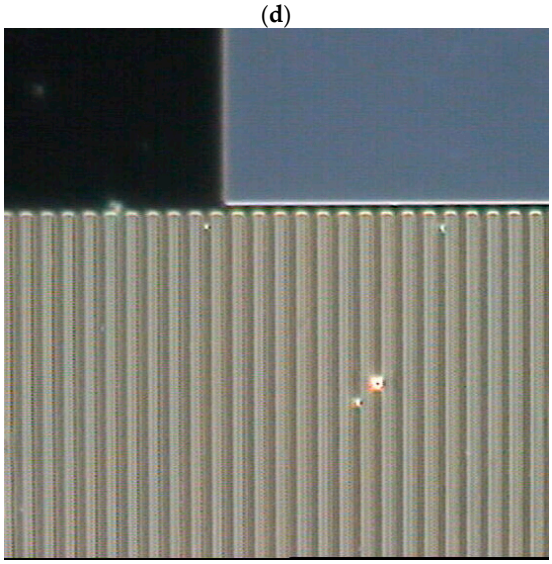

(**e**)

Figure 14. Exposures of the deposition of the PU-PLMA composite as the sensing nanometric layer. The coating results of the PU-PLMA composite showed a very distinct behavior compared to those obtained with the pristine sensing polymer. An improvement of the structural aspects of the resulting coating layer with the composites could be clearly observed. (**a**) Magnification 10× with DFM. (**b**) Magnification 10× with DFM. (**c**) Magnification 50× with BFM. (**d**) Magnification 50× with DFM. (**e**) Magnification 100× with DFM.

The combination with PU drastically changes the behavior of the deposition in comparison to the one obtained with the pristine PLMA (Figure 13). In the DFM expositions of 5- and 10-times magnification (Figure 14a,b), a clear change can be noted about the material distribution over the whole surface of the sensor element, and especially over the active area of the sensor in comparison with the results of the pristine PLMA deposition (Figure 13a). The exposures of 50-times magnification (Figure 14c,d) indicates the homogeneity of the coating layer of the PU-PBMA composite sensing material. The BFM exposure of 100-times magnification (Figure 14e) shows the presence of the coating material all over the interdigital structure of the active area of the sensor, also evidencing the homogeneity of the deposited sensing layer.

The value of the frequency shift for the PU-PLMA coating layer was the highest between all the other PU-Polymer composites, consistent with the fact that the coating layer of pristine PLMA also presented the highest value of frequency shift (Figure 2) among the pristine polymers as the sensing layer. The increase of the frequency shift also accounted for the respective increase of the attenuation value for the PU-PLMA composite, which was also the highest observed for the PU-Polymer composites (Figure 3).

3.8. PIB Sensing Layer

Figure 15 shows the exposures obtained for the coating layer using pristine PIB as the sensing material.

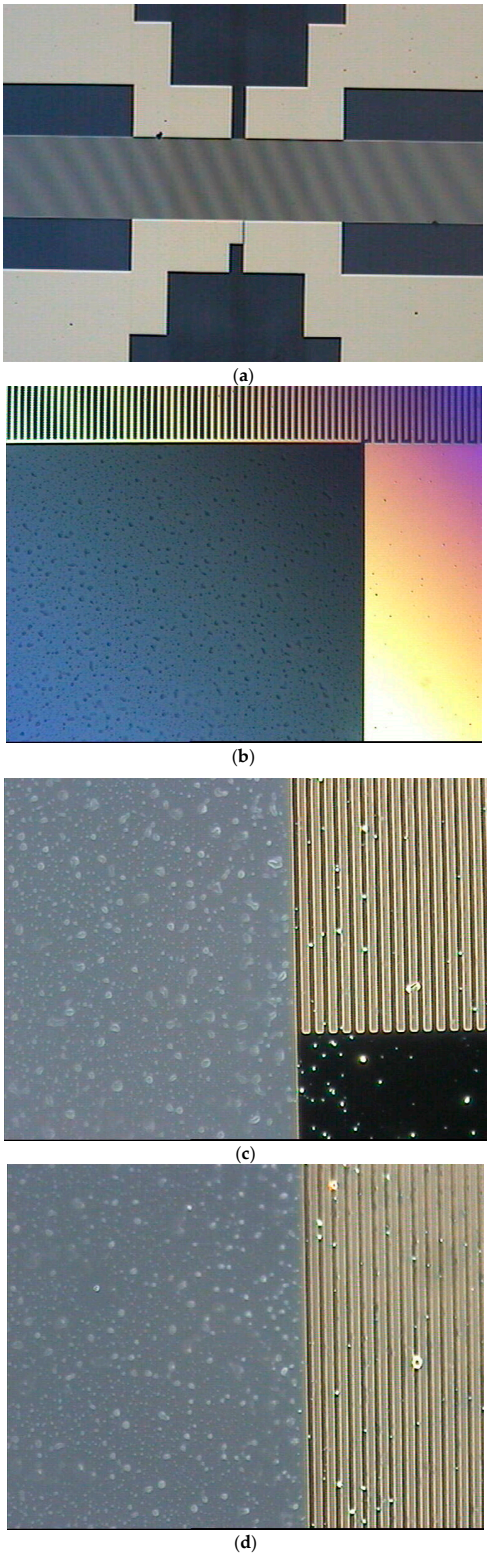

Figure 15. The exposures of the deposition of pristine PIB as the sensing layer showed distinct interactions with the regions of the sensor element surface. (**a**) Magnification 10× with DFM. (**b**) Magnification 50× with DFM. (**c**) Magnification 100× with BFM. (**d**) Sensitive sensor area magnification 100× with BFM.

The DFM exposure of 5-times magnification (Figure 15a) indicates a uniformity of the material distribution over the active area of the SAW sensor element by the pristine PIB coating. No pattern indicating a lack or an accumulation of the coating material can be observed. However, at DFM exposure of 50-times magnification (Figure 15b), the formation of droplets over the quartz region (largest blue region) can be seen, indicating a poor interaction with the quartz substrate. Over the interdigital structure and the gold contact pads, some droplets of the polymer can be seen, however much less than is observed in the quartz region (Figure 15c). The BFM exposure of 100-times magnification (Figure 15d) shows the contrast between the quartz region (large blue area) and the interdigital structure of the active sensor area, where the quartz region presents a higher occurrence of the droplets. Aside from the occurrence of some droplets over the sensor active area, no other inhomogeneity in the coating layer can be seen (Figure 15d).

In terms of the ultrasonic results, the attenuation value obtained with the pristine PIB deposition is lower than that obtained for the PLMA (Figure 13), indicating a better distribution of material and homogeneity of the coating layer of the pristine PIB over the sensor active area than that observed with pristine PLMA as the coating material.

3.9. PU-PIB Composite Sensing Layer

Figure 16 shows the images obtained for the coating layer obtained with the PU-PIB composite as the sensing material.

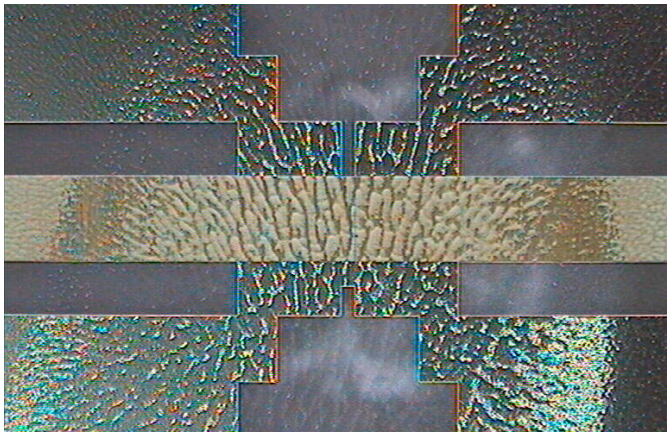

(**a**)

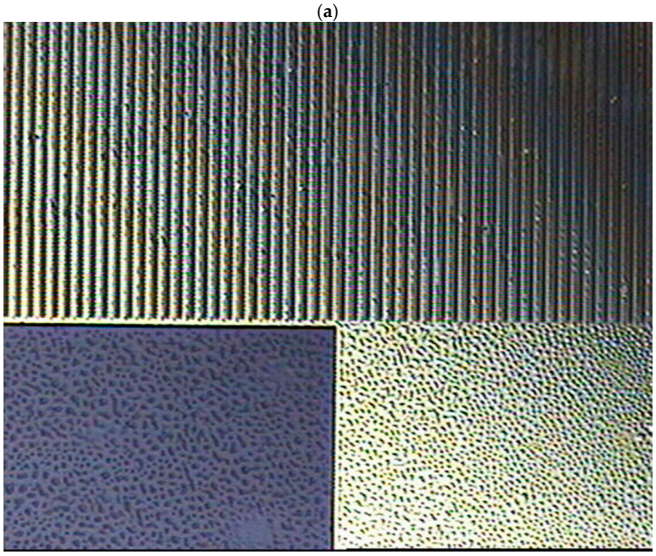

(**b**)

Figure 16. *Cont.*

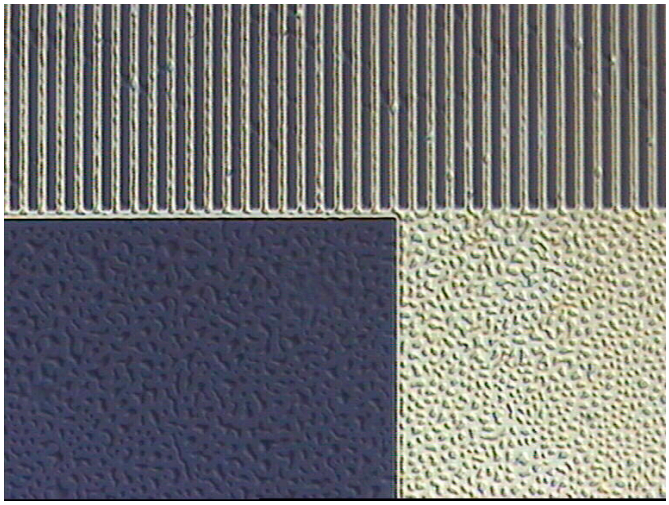

(**c**)

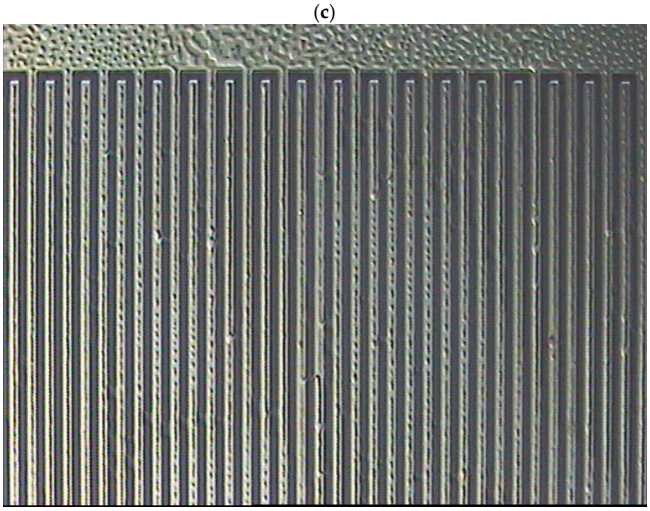

(**d**)

Figure 16. Exposures of the deposition of PU-PIB composite as sensing layer. The PU-PIB composite presented quite different properties in the structure of its sensing layer compared with those of its pristine former polymers. (**a**) Magnification 10× with DFM. (**b**) Magnification 50× with DFM. (**c**) Magnification 100× with DFM. (**d**) Sensitive sensor area detail—Magnification 100× with DFM.

The coating with the PU-PIB composite shows a quite different behavior than that observed by the deposition of pristine PIB as the coating material (Figure 15). The expected increase of the deposited material is confirmed by the value of the frequency shift (Figure 2). The changes of the properties of the PU-PIB composite coating material compared to the pristine PIB can be noted by the comparison of the DFM exposures of 5-times magnification of each deposition (Figures 15a and 16a). The DFM exposure of 50-times magnification shows a uniform material distribution over the three different substrates of the SAW sensor element, but is not homogeneous in all of them (Figure 16b). In the interdigital structure of the active sensor area, the deposition seems to show itself as more homogeneous than in the gold and quartz regions (Figure 16c). The deposition over the interdigital structure can be seen in more detail in the DFM exposure of 100-times magnification (Figure 16d).

3.10. PCTFE Sensing Layer

The results of BFM and DFM obtained for the PCTFE as sensing material are shown in Figure 17.

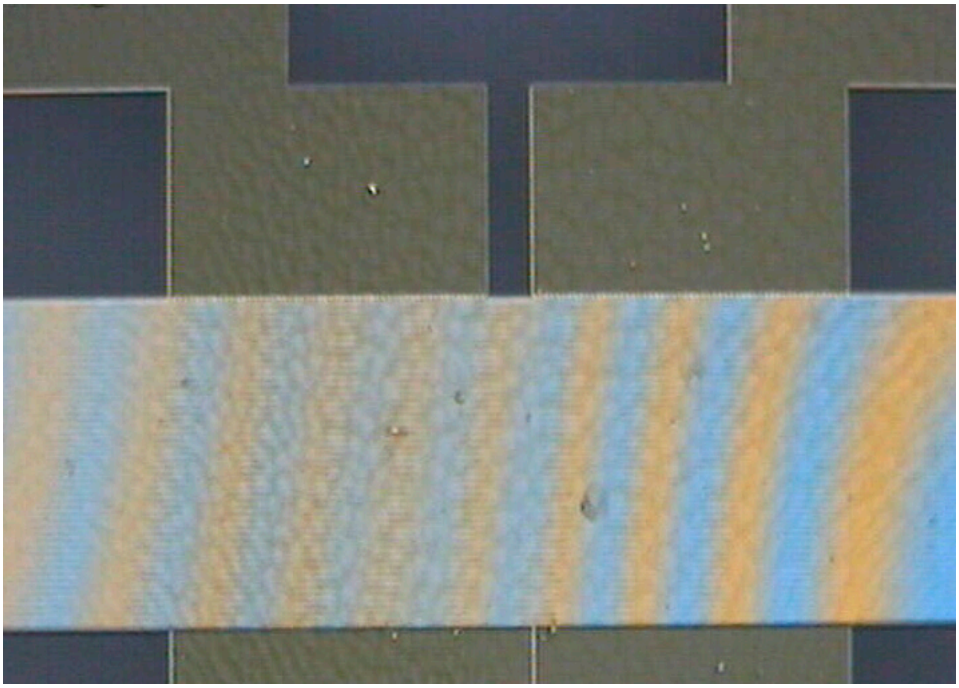

(**a**)

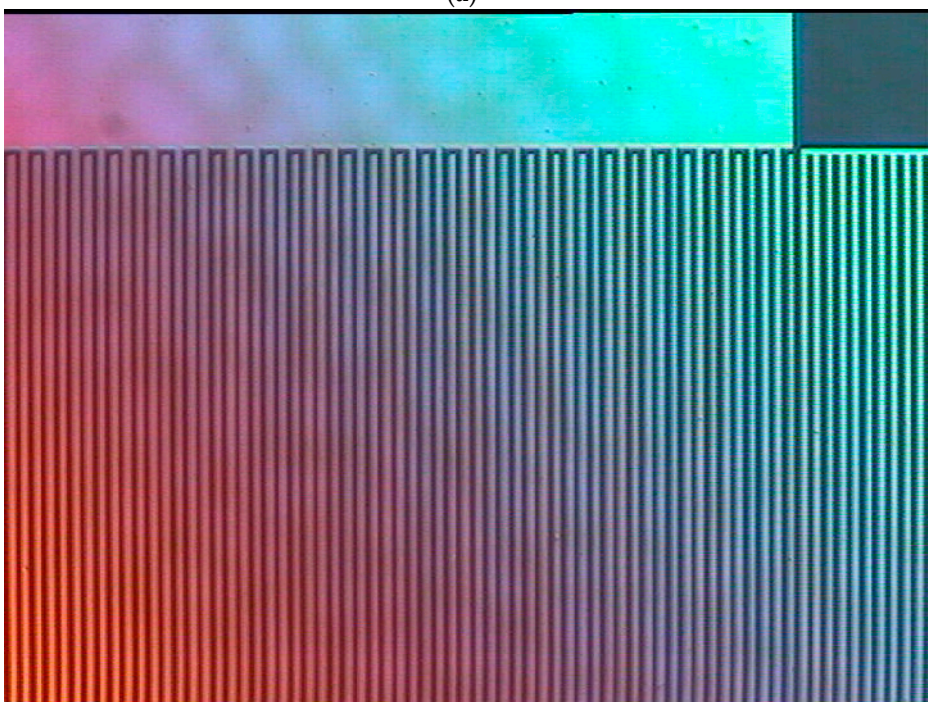

(**b**)

Figure 17. *Cont.*

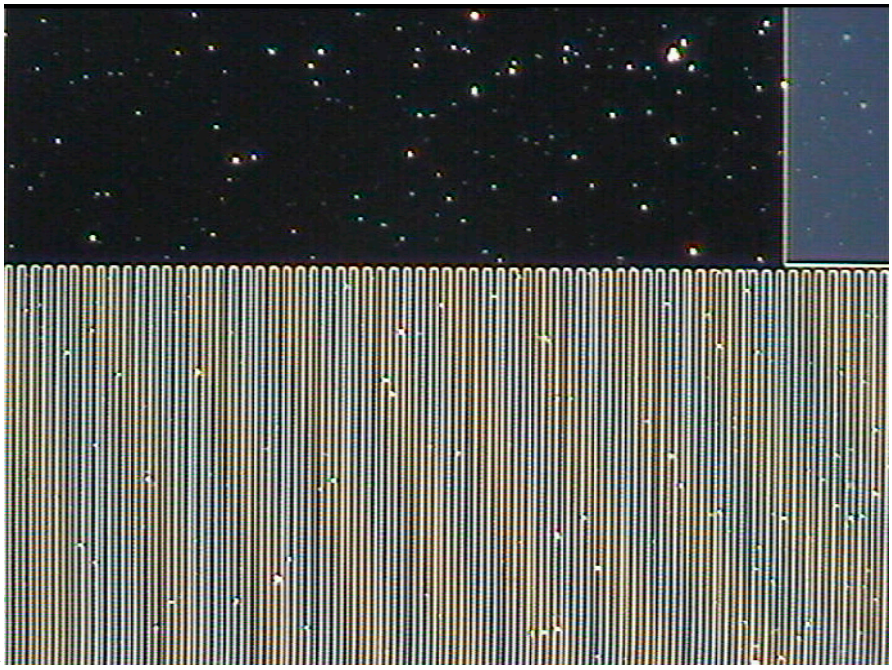

(**c**)

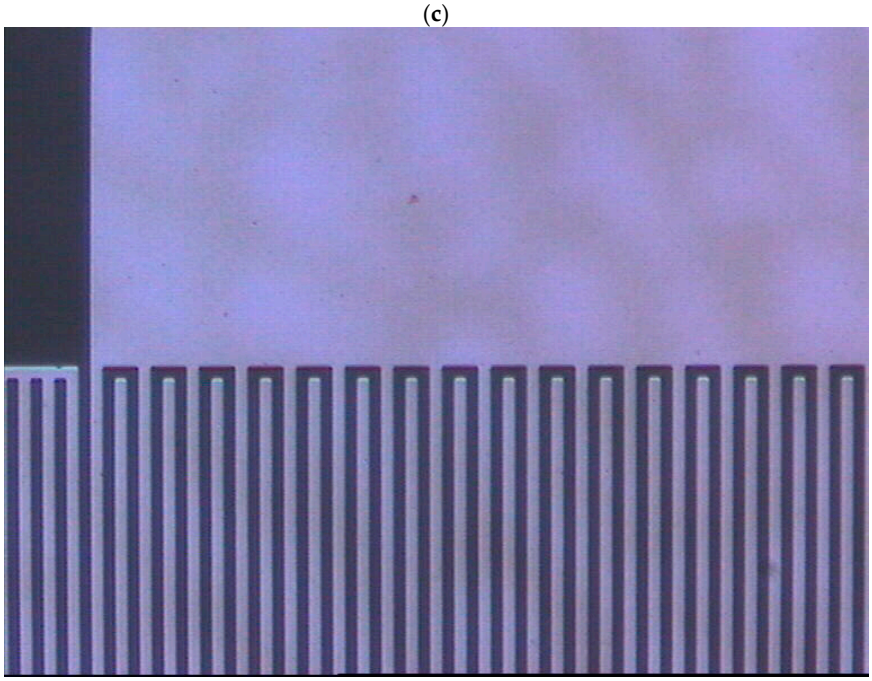

(**d**)

Figure 17. BFM and DFM exposures for the pristine PCTFE coating. The coating results for this distinct polymer in terms of its chemical constitution consequently presented a different pattern than those observed for the other investigated polymers. (**a**) Magnification 10× with DFM. (**b**) Magnification 50× with DFM. (**c**) Magnification 50× with BFM. (**d**) Magnification 100× with DFM.

The PCTFE deposition showed quite a different pattern than all the other polymers. The images of the deposited layer of this polymer show the presence of material over the whole surface of the piezoelectric sensor element, forming a pattern that seems to equally cover all the regions of the SAW sensor element (Figure 17a), being a quite distinct behavior from the other polymers investigated. The pattern can be visualized over the active area of the SAW sensor element by the 50-times magnification DFM exposure (Figure 17b). Aside from the pattern observed by the PCTFE coating, the layer does not show uniformities in

material distribution. In the same way, no lack of homogeneity of the layer can be observed, but just the formation of droplets as was also observed by other coating materials, as can be seen in the 50-times BFM exposure (Figure 17c). The DFM exposure of 100-times magnification shows a very regular deposition of coating material, where the pattern observed is also present (Figure 17d).

The PCTFE deposition presented the highest value of the frequency shift between all the polymers analyzed (Table 2), but not the highest attenuation. The quite different behavior of this polymer comes from its chemical composition. The voluminous halogen atoms lead to interactions of the PCTFE with the regions of the SAW sensor element surface that are different in comparison to the other polymers, which contain just the usual elements belonging to most of the organic functions. These factors shall also contribute to a correspondingly very distinct structure of the deposited layer with this polymer in comparison with the other polymers analyzed, and can be an explanation for the deviation in the results for the ultrasonic parameters for the PCTFE deposition in comparison to the other pristine polymers.

3.11. PU-PCTFE Composite Sensing Layer

The exposures obtained for the PU-PCTFE composite as the sensing material are shown in Figure 18.

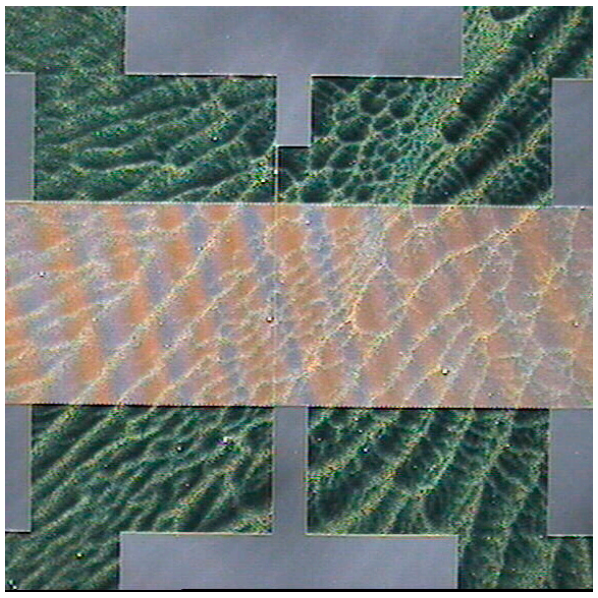

(**a**)

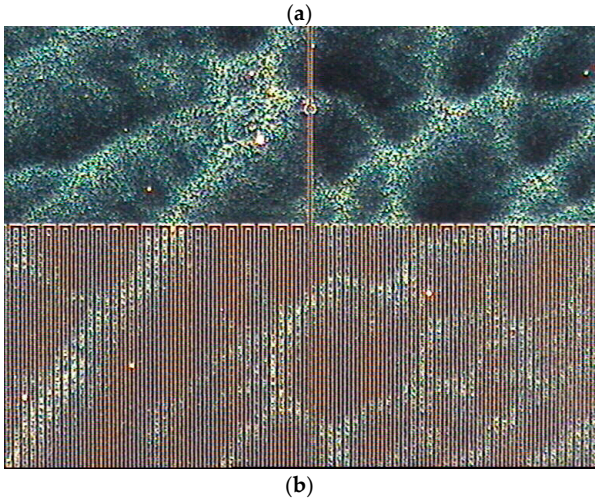

(**b**)

Figure 18. *Cont.*

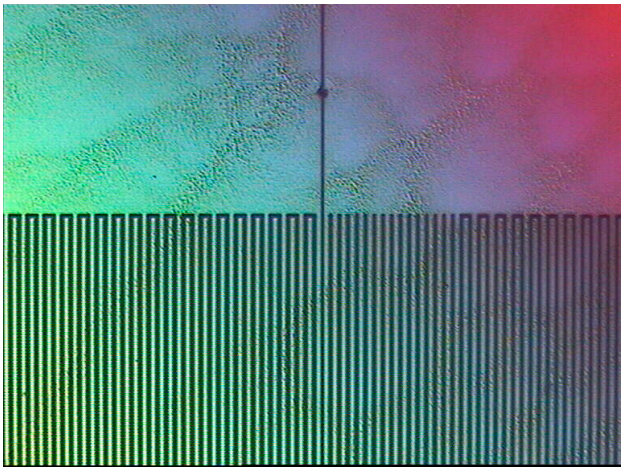

(**c**)

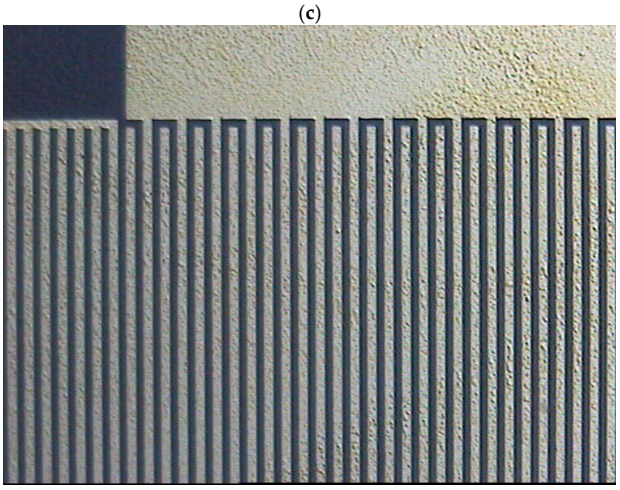

(**d**)

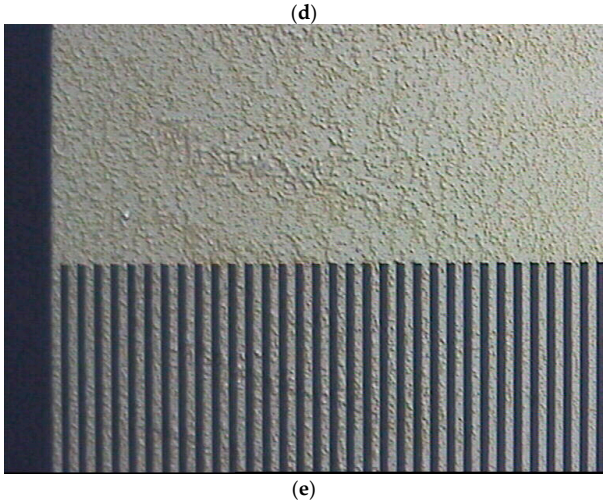

(**e**)

Figure 18. Exposures of BFM and DFM for the PU-PCTFE composite depositions. The coating results of the PU-PCTFE composite presented an overall pattern that appears to spread itself on the whole surface of the sensor element. (**a**) Magnification 10× with DFM. (**b**) Magnification 50× with BFM. (**c**) Magnification 50× with DFM. (**d**) Magnification 100× with DFM. (**e**) Magnification 100× with DFM.

The PU-PCTFE composite presented a very distinct behavior compared to that of the pristine PCTFE as the coating material. The composite material formed a very prominent pattern by the deposition, once again covering all the different regions of the SAW sensor element surface (Figure 18a). In the BFM exposure of 50-times magnification (Figure 18b),

the pattern observed seems to form a structure that spreads itself over the whole area of the SAW sensor element. The DFM exposure with the same magnification of the same region (Figure 18c) shows that the structure is formed by different concentrations of deposited material, and that this happens over all the regions, including the active area of the sensor. The inspection of the DFM exposures of 100-times magnification (Figure 18d,e) does make it possible to identify some regions with different concentrations of the deposited material. However, on average, at the scale of the interdigital structure, the material distribution appears to be more uniform, as the visual inspection of the lower magnifications suggest. As a matter of fact, on average, at the scale of the interdigital structures of the sensor active area, the material distribution is more uniform than that observed for the pristine polymer.

The value of frequency shift value for the composite was higher than that observed for the pristine PCTFE (Figure 2), as expected. But in this case, the increase in the frequency shift observed for the PU-PCTFE composite was smaller in comparison to those obtained for the other PU-polymer composites (Figure 2). For all the other PU-polymer composites, the increase of the polymer concentration of the coating solutions and the effect of a higher mass of the polymer deposited due to the formation of the composite with PU resulted in an expressive increase of the frequency shift and, consequently, in an increase in the attenuation values for the PU-polymer composites when compared to the values of the pristine polymers (Figures 2 and 3). The value of the attenuation for the PU-PCTFE composite contradicted the results observed for the other PU-Polymer composites. Aside from the observed unexpected lower increase of the frequency shift by the formation of the PU-composite, the value of the attenuation for the PU-PCTFE composite decreased. A possible explanation for this observation can be based on the difference between the properties of the pristine PCTFE and its PU composite. Due to the quite distinct chemical composition of this polymer, its combination with PU will form a material with properties that shall differ from the pristine polymer to a higher degree than those observed for the other analyzed polymer.

The analyses of the QAF (Figure 8) can also be associated with the results of the optical microscopy. The commented uniformity and homogeneity of the coating layers can be also ordered by the values of the QAF by taking the higher values of the QAF for the higher uniformity of the coating layer observed by the BFM/DFM exposures, for both pristine polymer and PU-polymer composites as coating materials. In the case of the pristine polymer, higher values of the QAF were found for the PU and PBMA coatings, coinciding with the BFM/DFM analysis where those coatings were the most uniform and homogeneous. The results of the microscopic observations agree with the order obtained for the QAF, with the uniformity of the coating decreasing in the sequence PIB < PLMA < PCTFE, as observed in the optical microscopy analysis.

Figure 9 orders the different coating materials according to their capacity to enhance the propagation of the acoustic wave through the surface of the SAW sensor, being PBMA and its PU-composite in the highest position and the PCTFE and its PU-composite in the lowest position.

The results showed that BFM and DFM optical microscopy can provide significant information about the real aspects of the deposited sensing layer, and the ultrasonic parameters can be correlated with the obtained exposures of the active sensor area.

These PU-polymer composites are new coating materials and were never used or studied before. It is also important to keep in mind that all the coating materials analyzed in this work provided fully operational SAW sensors that could be used in real applications and that demand coatings in the nanometric scale, making the structural analysis of the SAW sensing layers quite challenging.

4. Conclusions

The analysis of the frequency shift, attenuation, and the new defined QAF parameter successfully characterizes the sensing layers obtained with the pristine polymers and with the new PU-polymer composite coating materials. This allowed us to make inferences

about the interaction of the coating materials with the regions of the surface of the SAW sensor element. From the ultrasonic analysis, correlations between the results of the pristine polymer coating layers and those of the coating layers of the respective PU-polymer composites could be established, reinforcing the supposition that the PU-polymer composites are formed by a similar mechanism and that the resulting properties of their coating layers can be determined by their respective sensing polymers. The ultrasonic analysis could be, in turn, correlated with the BFM and DFM results, providing a nondestructive method to evaluate the real aspects of the obtained coating layers. The results showed that the material distribution can vary substantially depending on the chemical composition of the sensing material. The results confirmed the improvements obtained by the combination of the sensing polymers with PU to form composites with improved coating properties independent of the chemical constitution of the sensing polymer used. The exposures obtained with the BFM/DFM provided valuable information about how the coating material interacts with the different regions of the surface of the piezoelectric sensor element and especially could provide a visualization of the material distribution and of the homogeneity of the coverage over the active area of the sensor element. This will be crucial for the performance of the obtained SAW sensor. Therefore, the combination of BFM and DFM is shown to be both a very suitable method for the qualitative evaluation of the coating process to produce SAW sensors, as well as a very useful tool for the development of new coating materials for SAW sensor technology.

Author Contributions: Conceptualization, M.d.S.d.C. and M.R.; Methodology, A.V.; Software, A.V.; Validation, A.V.; Formal analysis, M.D.; Investigation, M.d.S.d.C.; Data curation, M.D.; Writing—original draft, M.d.S.d.C.; Writing—review & editing, M.d.S.d.C. and M.R.; Supervision, M.d.S.d.C.; Project administration, M.R. All authors have read and agreed to the published version of the manuscript.

Funding: The publication was funded by the Open Access Publication Fund of the Karlsruhe Institute of Technology.

Institutional Review Board Statement: Not applicable.

Informed Consent Statement: Not applicable.

Data Availability Statement: The data presented in this study are available on request from the corresponding author.

Conflicts of Interest: The authors declare no conflict of interest.

References

1. Yang, Y.; Dejous, C.; Hallil, H. Trends and applications of surface and bulk acoustic wave devices: A review. *Micromachines* **2023**, *14*, 43. [CrossRef]
2. Mandal, D.; Banerjee, S. Surface AcousticWave (SAW) Sensors: Physics, Materials, and Applications. *Sensors* **2022**, *22*, 820. [CrossRef]
3. Länge, K. Bulk and surface acoustic wave sensor arrays for multi-analyte detection: A review. *Sensors* **2019**, *19*, 5382. [CrossRef] [PubMed]
4. Misra, A.; Shahiwala, A. *Applications of Polymers in Drug Delivery*, 2nd ed.; Elsevier: Amsterdam, The Netherlands, 2020.
5. Nghiem, T.L.; Coban, D.; Tjaberings, S.; Gröschel, A.H. Recent advances in the synthesis and application of polymer compartments for catalysis. *Polymers* **2020**, *12*, 2190. [CrossRef] [PubMed]
6. Sun, Q.; Dai, Z.; Meng, X.; Wang, L.; Xiao, F.-S. Task-specific design of porous polymer heterogeneous catalysts beyond homogeneous counterparts. *ACS Catal.* **2015**, *8*, 4556–4567. [CrossRef]
7. Di Pietrantonio, F.; Benetti, M.; Cannatà, D.; Verona, E.; Palla-Papavlu, A.; Dinca, V.; Dinescu, M.; Mattle, T.; Lippert, T. Volatile toxic compound detection by surface acoustic wave sensor array coated with chemoselective polymers deposited by laser induced forward transfer: Application to sarin. *Sens. Actuators B Chem.* **2012**, *174*, 158–167. [CrossRef]
8. Sayago, I.; Fernández, M.J.; Fontecha, J.L.; Horrillo, M.C.; Vera, C.; Obieta, I.; Bustero, I. New sensitive layers for surface acoustic wave gas sensors based on polymer and carbon nanotube composites. *Sens. Actuators B Chem.* **2012**, *175*, 67–72. [CrossRef]
9. Yadava, R.D.S.; Kshetrimayum, R.; Khaneja, M. Multifrequency characterization of viscoelastic polymers and vapor sensing based on SAW oscillators. *Ultrasonics* **2009**, *49*, 638–645. [CrossRef]
10. Zhang, D.; Tong, J.; Xia, B. Humidity-sensing properties of chemically reduced graphene oxide/polymer nanocomposite film sensor based on layer-by-layer nano self-assembly. *Sens. Actuators B Chem.* **2014**, *197*, 66–72. [CrossRef]

11. Tai, H.; Zhen, Y.; Liu, C.; Ye, Z.; Xie, G.; Du, X.; Jiang, Y. Facile development of high performance QCM humidity sensor based on protonated polyethylenimine-graphene oxide nanocomposite thin film. *Sens. Actuators B Chem.* **2016**, *230*, 501–509. [CrossRef]
12. Raza, A.; Abid, R.; Murtaza, I.; Fan, T. Room temperature NH3 gas sensor based on PMMA/RGO/ZnO nanocomposite films fabricated by in-situ solution polymerization. *Ceram. Int.* **2023**, *49*, 27050–27059. [CrossRef]
13. Gu, Y.; Zhao, J.; Johnson, J.A. A (macro) molecular-level understanding of polymer network topology. *Trends Chem.* **2019**, *1*, 318–334. [CrossRef]
14. Tang, K.-T.; Li, C.-H.; Chiu, S.-W. An electronic-nose sensor node based on a polymer-coated surface acoustic wave array for wireless sensor network applications. *Sensors* **2011**, *11*, 4609–4621. [CrossRef] [PubMed]
15. Su, Y.-F.; Han, G.; Kong, Z.; Nantung, T.; Lu, N. Embeddable piezoelectric sensors for strength gain monitoring of cementitious materials: The influence of coating materials. *Eng. Sci.* **2020**, *11*, 66–75. [CrossRef]
16. Lowdon, J.W.; Diliën, H.; Singla, P.; Peeters, M.; Cleij, T.J.; van Grinsven, B.; Eersels, K. MIPs for commercial application in low-cost sensors and assays–An overview of the current status quo. *Sens. Actuators B Chem.* **2020**, *325*, 128973. [CrossRef]
17. Hu, J.; Qu, H.; Chang, Y.; Pang, W.; Zhang, Q.; Liu, J.; Duan, X. Miniaturized polymer coated film bulk acoustic wave resonator sensor array for quantitative gas chromatographic analysis. *Sens. Actuators B Chem.* **2018**, *274*, 419–426. [CrossRef]
18. Palla-Papavlu, A.; Voicu, S.I.; Dinescu, M. Sensitive materials and coating technologies for surface acoustic wave sensors. *Chemosensors* **2021**, *9*, 105. [CrossRef]
19. Jasek, K.; Pasternak, M.; Grabka, M.; Neffe, S.; Zasada, D. Deposition of Polymer Sensor Films on SAW Surface by Electrospraying Technology. *Arch. Acoust.* **2017**, *42*, 507–513. [CrossRef]
20. Rapp, M.; Voigt, A.; Dirschka, M.; dos Santos de Carvalho, M. The Use of Polyurethane Composites with Sensing Polymers as New Coating Materials for Surface Acoustic Wave-Based Chemical Sensors—Part I: Analysis of the Coating Results, Sensing Responses and Adhesion of the Coating Layers of Polyurethane–Polybutylmethacrylate Composites. *Coatings* **2023**, *13*, 1911. [CrossRef]
21. Dos Santos de Carvalho, M.; Rapp, M.; Voigt, A.; Dirschka, M. The Use of Polyurethane Composites with Sensing Polymers as New Coating Materials for Surface Acoustic Wave Based Chemical Sensors—Part II: Polyurethane Composites with Polylaurylmetacrylate, Polyisobutene, And Poly(Chlorotrifluoroethylene-Co-Vinylidene Fluoride): Coating Results, Relative Sensor Responses and Adhesion Analysis. *Coatings* **2024**, *14*, 778. [CrossRef]
22. Gao, P.F.; Lei, G.; Huang, C.Z. Dark-field microscopy: Recent advances in accurate analysis and emerging applications. *Anal. Chem.* **2021**, *93*, 4707–4726. [CrossRef] [PubMed]
23. David, M.; Arab, M.; Martino, C.; Delmas, L.; Guinneton, F.; Gavarri, J.-R. Carbon nanotubes/ceria composite layers deposited on surface acoustic wave devices for gas detection at room temperature. *Thin Solid Film.* **2012**, *520*, 4786–4791. [CrossRef]
24. Daugaard, A.E.; Jankova, K.; Hvilsted, S. Poly(lauryl acrylate) and poly(stearyl acrylate) grafted multiwalled carbon nanotubes for polypropylene composites. *Polymer* **2014**, *55*, 481–487. [CrossRef]